

UNCLASSIFIED

AD NUMBER

AD110592

CLASSIFICATION CHANGES

TO: UNCLASSIFIED

FROM: CONFIDENTIAL

LIMITATION CHANGES

TO:  
Approved for public release; distribution is unlimited.

FROM:  
Distribution authorized to U.S. Gov't. agencies and their contractors;  
Administrative/Operational Use; FEB 1956. Other requests shall be referred to Aeronautical Systems Div., Wright-Patterson AFB, OH 45433.

AUTHORITY

ASD ltr 19 Feb 1962 ; ASD ltr 12 Oct 1966

THIS PAGE IS UNCLASSIFIED

UNCLASSIFIED

AD 110 592

CLASSIFICATION CHANGED

TO: UNCLASSIFIED

FROM: CONFIDENTIAL

AUTHORITY:

ASD Ltr 19 Feb 62;

Public release Sec Ltr 12 Oct 66



UNCLASSIFIED

**Best  
Available  
Copy**

**NOTICE:** When government or other drawings, specifications or other data are used for any purpose other than in connection with a definitely related government procurement operation, the U. S. Government thereby incurs no responsibility, nor any obligation whatsoever; and the fact that the Government may have formulated, furnished, or in any way supplied the said drawings, specifications, or other data is not to be regarded by implication or otherwise as in any manner licensing the holder or any other person or corporation, or conveying any rights or permission to manufacture, use or sell any patented invention that may in any way be related thereto.

110592

**CONFIDENTIAL**

WADC TECHNICAL REPORT 56-97  
PART II  
ASIA DOCUMENT NO. AD 110592



(UNCLASSIFIED - Title)

THEORETICAL STUDIES ON THE PREDICTION  
OF UNSTEADY SUPERSONIC AIRLOADS ON ELASTIC WINGS

Part 2. Rules for Application of Oscillatory  
Supersonic Aerodynamic Influence Coefficients

Garabed Zartarian

MASSACHUSETTS INSTITUTE OF TECHNOLOGY

February 1956

WRIGHT AIR DEVELOPMENT CENTER

56WCLS-5098

MAR 5 1957

**CONFIDENTIAL**

NOTICE: THIS DOCUMENT CONTAINS INFORMATION AFFECTING THE  
NATIONAL DEFENSE OF THE UNITED STATES WITHIN THE MEANING  
OF THE ESPIONAGE LAWS, TITLE 18, U.S.C., SECTIONS 793 and 794.  
THE TRANSMISSION OR THE REVELATION OF ITS CONTENTS IN  
ANY MANNER TO AN UNAUTHORIZED PERSON IS PROHIBITED BY LAW.

**CONFIDENTIAL**

WADC TECHNICAL REPORT 56-27  
PART II  
ASTIA DOCUMENT NO. AD 110592

(UNCLASSIFIED - Title)  
THEORETICAL STUDIES ON THE PREDICTION  
OF UNSTEADY SUPERSONIC AIRLOADS ON ELASTIC WINGS  
Part 2. Rules for Application of Oscillatory  
Supersonic Aerodynamic Influence Coefficients

Garabed Zartarian

MASSACHUSETTS INSTITUTE OF TECHNOLOGY

February 1956

Aircraft Laboratory  
Contract AF33(616) - 2482  
Project 1370

Wright Air Development Center  
Air Research and Development Command  
United States Air Force  
Wright-Patterson Air Force Base, Ohio

**CONFIDENTIAL**

57AA

56WCLS-5098

13118

# CONFIDENTIAL

## FOREWORD

This report, which presents working rules and recommendations for flutter analysis using the aerodynamic-influence-coefficient method, was prepared by the Aeroelastic and Structures Research Laboratory, Massachusetts Institute of Technology, Cambridge 39, Massachusetts for the Aircraft Laboratory, Wright Air Development Center, Wright-Patterson Air Force Base, Ohio. The work was performed at the MIT under the direction of Professor H. Ashley, and the project was supervised by Mr. G. Zartarian. The research and development work was accomplished under Air Force Contract, No. AF 33(616)-2432, Project No. 1370 (Unclassified Title) "Aeroelasticity, Vibration and Noise," and Task No. 13473 (Unclassified Title) "Theoretical Supersonic Flutter Studies." Mr. Walter J. Mykytow of the Dynamics Branch, Aircraft Laboratory, is task engineer. Research was started on 1 July 1954. This report is part of a continuing effort in the flutter of aircraft structures at supersonic speeds. This is Part II of this report which is published in two separate parts.

The author, Mr. G. Zartarian, is indebted to Professor H. Ashley, Dr. P. T. Hsu and Mr. A. Heller for their contributions to the research. In addition, acknowledgements are due to Mr. G. Anitole for preparing the figures and to Mrs. B. Marks for typing the final manuscript.

This document, including the illustrations, is classified **CONFIDENTIAL** (excepting the title) because it contains the development of improved methods for conducting supersonic flutter analysis; hence more accurate flutter analyses for modern aircraft can be made.

# CONFIDENTIAL

## ABSTRACT

On the basis of investigations described in a preceding report (Ref. 1) and subsequent research, recommendations are made concerning methods of application of aerodynamic pressure or velocity potential influence coefficients to practical flutter analyses. Following a brief discussion of the relative merits of three basic types of elementary areas, working rules are given for wing planforms of principal interest. Simple illustrative examples have been included to clarify some of the details of the process. For the Mach box system of elementary areas, which is deemed to be the most satisfactory from the overall standpoint, formulas and tables of certain related functions are presented which will facilitate future tabulations of aerodynamic influence coefficients.

## PUBLICATION REVIEW

This report has been reviewed and is approved.

FOR THE COMMANDER:

*for*   
DANIEL D. McKEE  
Colonel, USAF  
Chief, Aircraft Laboratory

# CONFIDENTIAL

# CONFIDENTIAL

## TABLE OF CONTENTS

SECTION	PAGE
I Introduction	1
II Summary of the Relative Merits of the Three Basic Grid Systems	4
II.1 The Square Box	5
II.2 The Mach Box	6
II.3 The Characteristic Box	7
III Rules for Application of the Mach Box System To Planforms of Practical Interest	9
III.1 Purely Supersonic Planforms	9
III.2 Planforms with Supersonic Leading and Trailing Edges and with Side Edges Parallel to the Flight Direction	12
III.3 Planform with Subsonic Leading and Supersonic Trailing Edges	14
III.4 Planforms with Supersonic or Subsonic Leading Edges and Subsonic Trailing Edges	17
IV Determination of Downwash Distribution on the Diaphragm Region and Its Effect on the Airload Distribution	20
IV.1 Determination of the Downwash Distribution on the Diaphragm Region	21
IV.2 Determination of the Pressure or Velocity Potential Distributions on the Planform	28
IV.3 Aerodynamic Influence Coefficients Associated with Singular Downwash Distributions	28

# CONFIDENTIAL

## TABLE OF CONTENTS (Continued)

SECTION		PAGE
BIBLIOGRAPHY		33
APPENDIX A	Pressure and Velocity Potential Calculations	35
APPENDIX B	Determination of Downwash Distribution	47
APPENDIX C	Recommended Integration Techniques For Generalized Forces	56
APPENDIX D	Formulation of the Flutter Problem	61

# CONFIDENTIAL

## LIST OF ILLUSTRATIONS

	Page
Fig. III.1 Positioning of the Mach Box Grid System on a Purely Supersonic Planform	11
Fig. III.2 Positioning of the Mach Box Grid System on a Planform with Supersonic Leading and Trailing Edges and with Side Edges	14
Fig. III.3 Positioning of the Mach Box Grid System on a Planform with Subsonic Leading Edges and Side Edges	16
Fig. III.4 Positioning of the Mach Box Grid System on a Planform with All Edges Subsonic	18
Fig. IV.1 Illustrative Example for the Treatment of the Side Edge	21
Fig. IV.2 Characteristic Coordinate System	24
Fig. IV.3 Singular Downwash Distribution Near a Side Edge	25
Fig. IV.4 Illustrative Example for the Treatment of the Side Edge Including the Effect of Downwash Singularity	27
Fig. A.1 Square Grid System	36
Fig. A.2 Mach Grid System	36
Fig. B.1 Typical Spanwise Deflection Curve	48
Fig. B.2 Illustrative Example for Finding the Analytical Expression of the Deflection on a Cantilever Delta Wing	50
Fig. B.3 Lagrangian Interpolation for a Function of One Variable	52
Fig. B.4 Lagrangian Interpolation for a Function of Two Variables	54
Fig. C.1 Typical Chordwise Pressure Distribution Near a Side Edge (Steady-State Condition)	57
Fig. D.1 A Delta Wing Configuration with Lumped Masses	64

## LIST OF TABLES

Table A.1 Tabulation of $A_{\nu,\mu}^+$ , $A_{\nu,\mu}^-$ and $B_{\nu,\mu}$	43-45
Table A.2 Tabulation of $R_{\nu,\mu}$ for the Steady-State Case	46

# CONFIDENTIAL

## LIST OF SYMBOLS

$t$	Reference semi-chord
$t_j$	Streamwise dimension of a box
$C_{v,\mu}$	Pressure influence coefficient for Mach grid system $C_{v,\mu} = R_{v,\mu} + iI_{v,\mu}$
$C_d$	Structural influence coefficient
$C_1^{(w)}, C_2^{(n)}, C_d^{(w)}$	Pressure influence coefficients due to singular downwash as defined by Eqs. (4.10a-b) and Eqs. (4.13a-b)
$d$	Typical length in the characteristic coordinate system, taken to be equal to half the diagonal length of a Mach box
$f_j$	Deflection shape of the $j$ th-mode
$h$	Bending deflection (positive down)
$i$	$\sqrt{-1}$
$I_{v,\mu}$	Imaginary part of pressure influence coefficient for square grid system
$k$	Reduced frequency based on reference semi-chord, $k = \omega t / U$
$k_1$	Reduced frequency based on box size, $k_1 = \omega b_1 / U$
$\bar{k}_1, \bar{k}$	Modified reduced frequency, $\bar{k}_1 = \bar{k} = k_1 M^2 / \alpha^2$
$M$	Mach number
$p_{n,m}, \Delta p$	Pressure difference between upper and lower surfaces of thin wing (positive down) at box $(n,m)$
$\Delta p_i(x,y)$	Pressure difference distribution due to motion in the mode $i$
$Q_{ij}$	Generalized force
$q_r$	Generalized coordinate
$R_{v,\mu}$	Real part of pressure influence coefficient for square grid system
$r,s$	Characteristic coordinates (dimensional)
$t$	Time
$U$	Forward Velocity (supersonic)
$w$	Downwash (positive down)

# CONFIDENTIAL

## LIST OF SYMBOLS (Cont.d)

$\bar{w}_{\nu, \mu}$	Complex amplitude of downwash at box $(\nu, \mu)$
$\bar{w}_s$	Amplitude (strength) of singular downwash
$x, y$	Cartesian coordinates (dimensional)
PIC	Pressure influence coefficient (abbreviation)
VIC	Velocity potential influence coefficient (abbreviation)
$\alpha$	Angle of attack or torsional deflection of a beam-rod type wing (positive nose up)
$\beta$	$\sqrt{M^2 - 1}$
$\rho$	Density of the air
$\varphi$	Velocity potential
$\Delta\varphi_{n,m}$	Velocity potential difference between upper and lower surfaces of thin wing ( $\Delta\varphi = \varphi_U - \varphi_L$ ) at box $(n,m)$
$\Delta\varphi(x,y), \Delta\varphi_e$	Velocity potential difference at the trailing edge
$\Phi_{\bar{\nu}, \bar{\mu}}$	Velocity potential influence coefficient for Mach grid system
	$\Phi_{\bar{\nu}, \bar{\mu}} = \mathcal{R}_{\bar{\nu}, \bar{\mu}}^{(\varphi)} + i \mathcal{I}_{\bar{\nu}, \bar{\mu}}^{(\varphi)}$
$\Phi^{(s)}, \Phi_a^{(s)}, \Phi_e^{(s)}$	Velocity potential influence coefficients due to singular downwash as defined by Eqs. (4.10c-d) and Eqs. (4.13c-d)
$\omega$	Circular frequency of simple harmonic motion

**CONFIDENTIAL**

## SECTION I

### INTRODUCTION

In a preceding report (Ref. 1), the need for direct, systematic numerical methods for the determination of supersonic unsteady aerodynamic forces on wings was discussed with particular emphasis on the case of simple harmonic motion, which occurs in flutter calculations. Such an approach involves a division of the planform into small areas and use of so-called aerodynamic influence coefficients. Three alternative types of elementary areas were investigated with the ultimate aim of finding the particular one which would yield the most satisfactory results from an overall standpoint. Some of the aspects of this problem which had to be considered were the adaptability of the various grids to planforms of interest; limitations on the elementary box size, reduced frequency of the oscillations and Mach number; the relative ease of tabulating the aerodynamic coefficients; and finally the accuracies attainable in the generalized forces which enter the flutter equations.

In the assumed mode approach to the flutter problem, the quantities directly involved are the aforementioned generalized forces and not the pressure distributions themselves. Therefore, the ultimate aim is to determine the generalized forces satisfactorily. Evidently, if the pressure distributions are found accurately everywhere on the planform, the resulting generalized forces (which are weighted integrals over the planform area of these pressure distributions) will also be accurate. Cases appear, however, when the pressures at various control points obtained using any of the three elementary grids fluctuate appreciably from the true pressures. Fortunately, because of the averaging effects of numerical integrations over the planform, the resultant generalized forces in such cases will still be sufficiently accurate, provided the recommended rules in Sections III and IV are followed.

In Ref. 1 the primary interest was centered on the applicability of the so-called aerodynamic pressure influence coefficients (abbreviated from here on as PIC), because this type of influence coefficient appeared to be the most straightforward in applications. After completion of the research reported in Ref. 1, it was found that to determine generalized forces a better approach would be to make use of the velocity potential influence coefficient (abbreviated from here on as VIC). In all the applications made up to date, the VIC-method has proven itself to be superior to the PIC-method, and has indicated the

Manuscript released by the author February 1956 for publication as a WADC Technical Report.

**CONFIDENTIAL**

**CONFIDENTIAL**

following two important advantages:

- (1) The VIC-tabulation would require less than half the machine operations than those for the PIC.
- (2) For planforms with subsonic edges, and for a given accuracy, fewer boxes are needed with the VIC-method.

Because of the importance of this new approach, it is reported here in advance, pending the completion of detailed investigations on the VIC-method. Further applications of this method will be undertaken and reported on in the future. Although the rules stated in Sections III and IV are based primarily on the findings about the PIC-approach, they are still valid with minor modifications when employed in connection with the VIC.

Inasmuch as the so-called Mach box grid system offers advantages in many respects, especially for planforms with subsonic edges at  $M < \sqrt{2}$ , the emphasis has been placed on the use of this system. Rules have been devised to assure satisfactory results, with the maximum generality and simplicity, whenever possible. Additional rules and techniques are also presented to meet the requirements of specific planforms and edge configurations. For instance, a method is presented in Section IV to account for the effect of the singular downwash at side edges on the airloads. Such refinements, which improve markedly the accuracies of the final results (Ref. 1), have been recommended for use whenever they are needed and can be incorporated conveniently.

Although not specifically stated, some of these rules are applicable to the square grid system, for which tables of the PIC's are already available (Ref. 2).

At relatively high Mach numbers, say  $M > 2.5$ , the recently developed "piston theory" is promising for many types of planforms. Preliminary investigations (Refs. 3,4) have indicated that, at these Mach numbers, airloads on two-dimensional or purely supersonic airfoils with small to moderate sweep can be predicted satisfactorily. An extension to the three-dimensional case seems feasible. The accuracy of such predictions improves as the Mach number is increased. In view of the simplicity of this theory, its use, whenever applicable, is preferred for this high Mach number range.

In Appendix D, a simple flutter problem is formulated to illustrate the various steps in applying either of the two types of influence coefficients. If the flutter problem is to be solved by means of a high-speed digital computer, two alternative ways can be followed in feeding the aerodynamic influence

**CONFIDENTIAL**

# CONFIDENTIAL

coefficients into the machine: (1) to store the required table of influence coefficients which have already been calculated elsewhere, or (2) to store the sub-routines which generate the influence coefficients whenever they are called for. The final choice as to which process should be employed depends mainly on the storage capacity and the speed of the computer, and the ease of programming.

This report is intended primarily to supply working rules in the use of the Mach grid system for aeroelasticians interested in solving practical flutter problems. No effort has been made here to substantiate these rules, since they have been extensively discussed in Ref. 1. It should be emphasized here that these rules were arrived at by experience on a limited number of representative trial cases, with due consideration being given to compromises between desired accuracy and practicability of the method. Therefore, these rules do not guarantee a given accuracy, and their use does not necessarily result in a uniform accuracy for all types of planforms. They are expected, however, to yield acceptable calculated airloads for flutter analyses.

With the VIC-method, which is concluded to be the better approach, it is felt that it is now unnecessary to tabulate aerodynamic influence coefficients. Using one of the tables in this report (page 45), the procedure for obtaining the VIC's according to the approximate expressions is quite straightforward. Engineers using the present method can have these tabulated in a very short time for any Mach number and reduced frequency. Most flutter calculations will be carried out on high-speed digital computing machines, on which very simple subprograms can be devised for instantaneous generations of the coefficients as needed.

Under an extension of the subject contract, the following investigations are contemplated:

- (1) The possibility of using a subdivision technique for partial boxes at the leading and trailing edges.
- (2) A simplified procedure for handling the downwash singularity near subsonic leading and side edges. It appears that, with certain assumptions, it is feasible to formulate a general refinement of this type for subsonic leading and side edges.
- (3) Applications of these methods to wings of various planforms (straight tapered, delta and swept), for which experimental data are available.

# CONFIDENTIAL

# CONFIDENTIAL

## SECTION II

### SUMMARY OF THE RELATIVE MERITS OF THE THREE BASIC GRID SYSTEMS

In a preceding report (Ref. 1), several numerical techniques for the calculation of airloads on oscillating wings in supersonic flow were studied, all of which have their origin in a suggestion by Pines (Ref. 5). Briefly, this approach starts with the definition of the aerodynamic influence coefficient, according to which the pressure (or the velocity potential) at any point  $(x, y)$  on the planform is related to the values of the vertical velocity ("downwash") on elementary areas ("boxes") located in the region bounded by the forward Mach lines emanating from  $(x, y)$ . With certain specific exceptions, such as the downwash singularity just off a side edge, each aerodynamic influence coefficient represents the pressure (or the velocity potential) induced at  $(x, y)$  by a constant unit downwash over a particular elementary area, with zero downwash over all other such areas. In view of the linearity of the theory, the total pressure (or the total velocity potential) at  $(x, y)$  is approximately equal to the sum of the influence coefficients for all boxes affecting that point, each one weighted with an appropriately averaged downwash for its box. When the quantity of interest at  $(x, y)$  is the pressure, one uses the pressure influence coefficients (PIC). When this quantity is the velocity potential ( $\varphi$ ) one must employ the velocity potential influence coefficient (VIC).

Three basic shapes of elementary areas were investigated, in connection with the PIC-method, with the objective of determining the overall practicability of each in numerical applications.

1. The square box (the shape originally proposed by Pines);
2. The Mach box, which is a rectangle with its diagonals parallel to the Mach lines;
3. The characteristic box, which is a rhombus bounded by four Mach lines.

These alternative schemes were applied to simple trial cases for which analytic solutions are known. In so doing, several relevant points were established regarding the suitability of

# CONFIDENTIAL

each of the grid systems. Advantages and disadvantages associated with each one were recognized.

Before attempting to apply the influence coefficient methods to particular problems, it is desirable to understand clearly the relative merits of each box shape, so as to make a judicious choice. For this purpose a summary of the conclusions reached according to the investigations for the pressure influence coefficients (Ref. 1) is now presented. In general, the conclusions reached there are expected to apply for the VIC-method as well.

## II.1 The Square Box

### Advantages:

1. Tabulations of the pressure influence coefficients are already available for a 20 x 20 grid system (Ref. 2). The number of boxes that can usually be taken in the chordwise direction (20) is large enough for most purposes. These boxes may nearly always be used satisfactorily for purely supersonic planforms (e.g., the wide deltas). They may also be used for planforms with subsonic edges when  $M > \sqrt{2}$ .
2. The grid system, and therefore the pressure (or velocity potential) and downwash control points, remain fixed when the Mach number is varied. This is a desirable feature since it facilitates the necessary numerical integrations for the generalized forces.

### Disadvantages:

1. This system cannot be used for planforms having subsonic edges when  $M < \sqrt{2}$ .
2. On the basis of trial examples with the VIC, this method is very likely to supersede entirely the original PIC-method. The computational work of tabulating the VIC's according to exact or approximate expressions far exceeds that for the other two types of boxes.
3. The effect of the downwash singularity near a side edge cannot be easily incorporated, when this refinement is needed.
4. If exact expressions (as far as the frequency is concerned) for the influence coefficients are used instead of the approximate ones given by Pines (Ref. 6), fewer boxes may be sufficient in some instances.

# CONFIDENTIAL

Tabulations using these exact expressions are much more complicated, however, than the corresponding ones for the Mach box (see Appendix A).

5. Unless one tabulates the contributions due to "half square boxes," the condition of zero pressure (or equivalently zero velocity potential) cannot be satisfied on a streamwise side edge, with the result that lift and moment distributions cannot be made to vanish identically at such an edge.

6. The centers of boxes do not fall on the Mach line which separates the purely supersonic and the mixed regions near a side edge. A refined chordwise integration technique for calculation of generalized forces (with the PIC-method), as illustrated in Appendix C, therefore cannot be used.

## II.2 The Mach Box

### Advantages:

1. This system can be used conveniently and with satisfactory accuracy for planforms having subsonic edges and for all supersonic Mach numbers, ( $M > 1.2$ ).
2. The singularity in downwash at a side edge may be accounted for.
3. Tables based on Watkin's exact expressions for the influence coefficients (PIC or VIC) are rather simple to compute (See Appendix A).
4. Pressures are obtained on the Mach line which separates the purely supersonic and the mixed regions near a side edge. This is desirable if the integration technique of Appendix C is needed (for the PIC-method).

### Disadvantages:

1. Unless one tabulates the contributions due to "half Mach boxes," the condition of zero pressure (or zero velocity potential) cannot be satisfied on a side edge, with the result that lift and moment distributions cannot be made to vanish identically at such an edge.
2. The control point locations vary when the Mach number is changed, and hence the downwashes must be recalculated for each Mach number. However, this task is

# CONFIDENTIAL

relatively easy using interpolation or equivalent procedures derived in Appendix B. The numerical integration formulas for the generalized forces must be devised for each Mach number; again, this is relatively simple and constitutes only a very small percentage of the total computational effort.

3. For large Mach numbers, say  $M \geq 2.5$ , many spanwise boxes must be taken to ensure a sufficient number in the chordwise direction. However, at these high Mach numbers, almost all of the present planforms will have supersonic edges, and the number of chordwise boxes need not be too large. Also, for  $M \geq 2.5$ , it is recommended that the much simpler "piston theory" (Refs. 3,4) be used whenever applicable.

## II.3 The Characteristic Box

### Advantages:

1. This system can be used for planforms having subsonic edges and for all supersonic Mach numbers, ( $M \geq 1.2$ ).
2. The singularity in downwash at a side edge may be accounted for.
3. Tabulations (PIC or VIC) are not expected to be too difficult, although they will be more laborious than those for Mach boxes.
4. The condition of zero pressure (or zero velocity potential) can be satisfied at discrete points on a side edge.
5. Pressures are obtained on the Mach line separating the purely supersonic and the mixed regions near a side edge (PIC-method).

### Disadvantages:

1. The control point locations vary when the Mach number is changed. (This is a minor objection as stated in connection with the Mach box.)
2. As in the case of the Mach box, for  $M \geq 2.5$  many spanwise boxes must be taken to ensure a sufficient number of boxes in the chordwise direction.

## CONFIDENTIAL

3. Although at first glance this box system might appear quite versatile for swept leading edges, experience has shown that (except for a leading edge exactly parallel to a Mach line) it yields poorer results than when the leading edge is represented by a jagged boundary composed of lines perpendicular and parallel to the flow. To represent the leading edge in the latter fashion, when characteristic boxes are being employed, tables must be calculated of aerodynamic influence coefficients for "half-rhombic" or triangular boxes. Furthermore, experience indicates that when a wing has a streamwise side edge or a swept leading edge and the downwash varies appreciably in the chordwise direction, it is desirable to have influence coefficients tabulated for "quarter-rhombic" boxes. These requirements increase the total number of entries in the tables by a factor of four, which is a serious drawback relative to the other two-box methods. These problems are discussed in detail in Ref. 1.

It should be noted that some of the above advantages and disadvantages are based on the condition of keeping to a minimum the computational labor to determine satisfactorily the generalized forces; (this implies keeping the number of boxes on the planform to a minimum). If many more than the required number of boxes are taken, some of the refinements, such as the inclusion of the effect of side-edge downwash singularity or the use of the more elaborate integration techniques of Appendix C, may become unnecessary. Therefore, for these cases, some of the advantages and disadvantages mentioned above may become insignificant.

From experience to date, it appears that the Mach box system rates most favorably for the majority of practical applications. Accordingly it is recommended as the basis for future tabulations of supersonic aerodynamic influence coefficients.

# CONFIDENTIAL

## SECTION III

### RULES FOR APPLICATION OF THE MACH BOX SYSTEM TO

#### PLANFORMS OF PRACTICAL INTEREST

In order to carry out flutter analyses efficiently using the Mach box scheme, certain working rules, which are given below for specific planforms and edge conditions, must be followed. It is possible to enunciate more general rules which apply for all combinations of planform and Mach number. The latter set would allow the analyst less freedom of choice in a particular case, however, since it would overlook some of the possible simplifications and refinements.

Planforms of current interest may be classified into three categories: the straight tapered, the sweptback tapered, and the triangular. As the Mach number is varied, each of these planforms may exhibit supersonic or subsonic edges, the former being characterized by a sweep angle less than that of a Mach line, and conversely. For different ranges of Mach number, it is necessary to follow different sets of rules.

Although these rules are based on the experience gained by carrying out examples using the PIC's (Ref. 1), a few trial calculations on some of these examples with the use of the VIC's have indicated that most of the rules still apply, with increasing resultant accuracies for planforms with subsonic edges. These rules should therefore be adopted for both methods, unless specifically stated otherwise.

#### III.1 Purely Supersonic Planforms

The following rules apply for purely supersonic planforms (planforms with no subsonic leading or trailing edges and no side edges; e.g., the wide delta).

##### Rules:

1. The dimensions of the elementary areas to be distributed over the planform are found from the condition that, for the highest Mach number to be considered in the analysis, a minimum of eight boxes chordwise along the root chord is recommended. When possible, the spanwise dimension of the boxes should be kept constant, because then the spanwise locations of the control points do not vary, and the overall width of the grid of boxes bears a fixed

# CONFIDENTIAL

relation to wingspan. As the Mach number is decreased, the resulting reduction of the chordwise box dimension  $b_i$  causes only a moderate variation of the reduced frequency

$$\bar{R}_i = (\omega b_i / U) (M^2 / \beta^2)$$

for a given frequency of oscillation  $\omega$ . However, if the range between the maximum Mach number,  $M_{max}$  and the Mach number when any of the edges becomes sonic,  $M_{son}$  is large, the number of chordwise boxes may become quite high. If eight boxes are taken for  $M_{max}$ , then for  $M_{son}$  there will be

$$8 \frac{\sqrt{M_{max}^2 - 1}}{\sqrt{M_{son}^2 - 1}} \text{ boxes.}$$

If this number becomes impractical on account of limitations of tabulations or the capacity of the computing machine, a reduction of the number of spanwise boxes is recommended at the lower Mach numbers. In any case, no less than eight boxes along the root chord should be employed. For most of these types of planform the application of this rule will also ensure a sufficient number of spanwise boxes.

2. The number of chordwise boxes is further governed by two factors: the accuracy of the tabulations and the most sinuous assumed mode shape.

a. If approximate formulas for the influence coefficients (Appendix A) are used, the number of chordwise boxes must be chosen such that

$$\bar{R}_i = \frac{\omega b_i}{U} \frac{M^2}{\beta^2} \leq 0.3 \quad \text{Eq. (3.1)}$$

b. In the evaluation of the generalized forces, associated with the assumed mode type of flutter analysis, the mode which is the most sinuous in the chordwise direction will determine the maximum tolerable box size. A minimum of six boxes per "half wave length" of this mode shape should be used.

3. After the box size is determined by conditions 1 and 2, a grid system can be constructed. Although no specific rule for proper positioning of this grid system on the planform can be given for all cases, the example shown in Fig. III.1 will serve as a guide. The leading edge of the actual planform will be replaced by a jagged line. Therefore, the

# CONFIDENTIAL

chordwise positioning of the box system with respect to the leading edge must be such that the leading edge area of the planform left out by the grid system is approximately equal to the area outside the planform taken in by the grid. Since the trailing edge is supersonic, no particular relationship between that line and the box centers adjacent to it need be imposed.

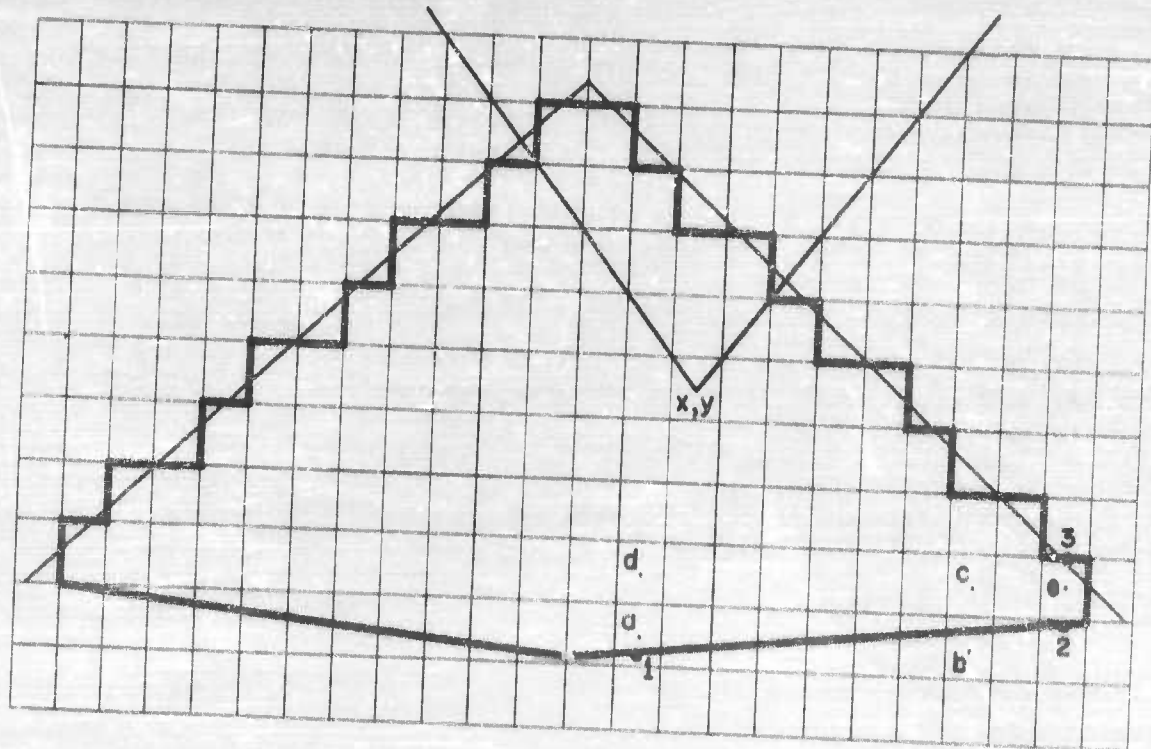


Fig. III.1 Positioning of the Mach Box Grid System on a Purely Supersonic Planform

4. According to Rule 3, the actual planform is replaced by an approximate one composed of boxes with centers on the planform. Near the trailing edge, all boxes partially on the planform, regardless of the locations of their centers, are to be included. Two types of such partial boxes appear. Referring to Fig. III.1, box *a* has its center on the planform, while box *b* has its center behind the trailing edge. For box *a*, the pressures (or the velocity potential  $\Delta\psi$ ) and the associated weighting factors for the generalized forces (Appendix C) can be computed like

# CONFIDENTIAL

those for any other complete box. For box  $b$ , the pressures (or  $\Delta\psi$ ) and the weighting factors should be assumed equal to the corresponding ones for the adjacent upstream box  $c$ . For each partial box, its contribution to the generalized force must be multiplied by the ratio of its area on the planform to its total area. In addition, when dealing with the VIC-method, it is necessary to determine  $\Delta\psi$  at points on the trailing edge. This is accomplished by extrapolation. For instance, the  $\Delta\psi$  at point 1 is found by linear extrapolation using the values at the centers of boxes  $a$  and  $d$ ; the  $\Delta\psi$  at point 2 is found by linear extrapolation using the value of zero for point 3 and the calculated value for the center of box  $e$ .

5. With the pattern of boxes over the planform completely established, the (complex) downwash amplitude at the center of each box is found from the mode shape of simple harmonic motion. Appendix B discusses this operation. With the downwash amplitude at the center of each box known, the (complex) amplitude of pressure difference or of the velocity potential difference between the upper and lower surfaces of the wing

$$(\bar{p} = \Delta\bar{p} = \bar{p}_u - \bar{p}_l, \Delta\bar{\psi} = \bar{\psi}_u - \bar{\psi}_l)$$

can be computed at each control point from either Eq.(A.6) or Eq. (A.8) of Appendix A.

6. The rectangular integration rule is to be applied for generalized force integrations. The pressures or  $\Delta\psi$ 's and the weighting factors are assumed to be constant over each box. The generalized force can be computed from Eq. (C.10) or Eq. (C.14) of Appendix C, or from equivalent formulas.

## III.2 Planforms with Supersonic Leading and Trailing Edges and with Side Edges Parallel to the Flight Direction

Associated with any subsonic edge, such as a side edge, there are two special regions to be considered. These are the so-called "mixed region," which is the portion of the planform influenced by the subsonic edge and the so-called "diaphragm region" off the planform where disturbances exist. The condition of zero pressure difference must be imposed over the diaphragm region. Near a side edge parallel to the flow, this condition is identical with the requirement that the difference in the velocity potential be zero at all points of the diaphragm. From either of these conditions, the unknown downwash on this region can be calculated. Furthermore, it is known that the downwash distribution has a square-root singularity as the subsonic edge is approached from the diaphragm region. Two

# CONFIDENTIAL

alternatives in calculating the effect of this diaphragm region on the mixed region may be followed:

Alternative 1: If the unknown downwash over each diaphragm box is assumed constant, the downwash over such boxes may be computed by satisfying the condition of zero pressure (or zero  $\Delta\varphi$ ) at the centers. Once these downwashes are determined, the diaphragm boxes may then be treated like any other box on the planform. As a general rule, this is satisfactory when there is a minimum of ten boxes along the side edge. It should be pointed out that with ten boxes and the VIC-method, one obtains better accuracy than with the same number of boxes and the PIC-method, so that this minimum may be lowered somewhat when the former is employed.

Alternative 2: When fewer than this minimum are employed along the side, the assumption of constant downwash over each diaphragm box adjacent to the side edge is not adequate unless the mixed region is small compared to the plan area and contributes a small portion to the generalized force. In most practical cases, however, the loadings near the side edge will be quite large since the maximum deflections during flutter occur near the tip. Then one must incorporate the effect of the downwash singularity. This procedure is illustrated in Section IV.

Rules: The rules given for purely supersonic planforms apply in general also to this class of planforms. These are supplemented by the following additional rules:

1. The approximate box size dictated by the conditions of Section III.1 should be adjusted so that there will result an integral number of boxes across the span.
2. Referring to Fig. III.2, the actual side edge  $ab$  is replaced by  $a'b'$ . Consequently, the actual mixed region  $abc$  must be replaced by  $a'bc'$ .
3. The diaphragm region  $ba'd$  is to be represented by complete boxes if the downwashes over such boxes are assumed constant. Its leading edge is no longer a Mach line but the jagged line formed by the boundaries of the foremost boxes.
4. The pressures or the velocity potentials over the mixed region  $a'bc'$  are to be found according to Section IV.

CONFIDENTIAL

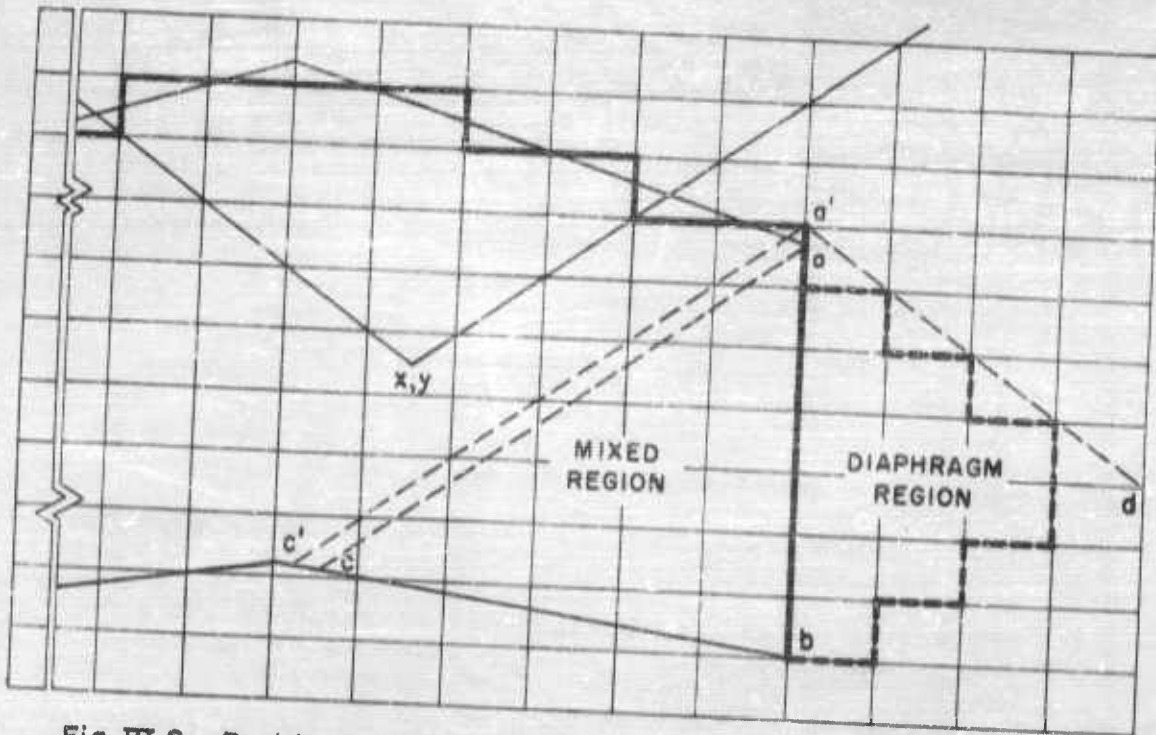


Fig. III.2 Positioning of the Mach Box Grid System on a Planform with Supersonic Leading and Trailing Edges and with Side Edges

5. If few chordwise boxes are employed near the side edge, the integration technique of Appendix C is to be used when computing generalized forces, in place of the simple rectangular rule. This refinement is necessary only with the PIC-method.

### III.3 Planform with Subsonic Leading and Supersonic Trailing Edges

When a planform with subsonic leading edges is considered, two serious difficulties arise. First, the replacement of the leading edge by a jagged line causes large fluctuations of the pressure or of the velocity potential about their true values over each box. Secondly, in the diaphragm region ahead of the leading edge, there exists a singular downwash distribution similar to that near a side edge. Unlike the side edge case, this effect cannot be incorporated successfully in the theory. Both of these difficulties dictate the use of a large number of boxes.

CONFIDENTIAL

# CONFIDENTIAL

## Rules:

1. A minimum of twelve boxes along the mid-span chord is required.
2. Rules 2, 3, 4 of Section III.1 apply. Figure III.3 is furnished as an example of how a typical planform might be overlaid with Mach boxes.
3. If side edges exist, the approximate box size dictated by previous conditions should be adjusted so that there will result an integral number of boxes across the span. Again the spanwise dimension should be kept constant as the Mach number is varied. At the lowest Mach numbers more than twelve chordwise boxes will then be present, and this is desirable because the leading edge becomes "more subsonic."
4. The diaphragm region is comprised of complete boxes in the disturbed region off the planform, as shown in Fig. III.3.
5. With the pattern of boxes over the planform completely established, the (complex) downwash amplitude at the center of each box on the planform is found from the mode shape of simple harmonic motion (Appendix B).
6. With the downwash amplitude at the center of each box on the planform known, the constant downwash amplitude over each box in the diaphragm region is determined from the condition of zero pressure (or zero  $\Delta\psi$ ) at the centers of diaphragm boxes, according to Section IV.1.
7. With the downwash amplitudes at the centers of all boxes known, the (complex) amplitude of pressure difference (or  $\Delta\psi$ ) between the upper and lower surfaces can be computed at each control point on the planform from Eq. (A.6) or Eq. (A.8) of Appendix A.
8. The potentials at trailing edge points are found by extrapolation as in rule 4, Section III.1.
9. The rectangular rule is to be applied for generalized force integration, the pressures (or  $\Delta\psi$ ) and the weighting factors being assumed constant over each box. The generalized forces can be computed from Eq. (C.10) or Eq. (C.14) of Appendix C.

**CONFIDENTIAL**

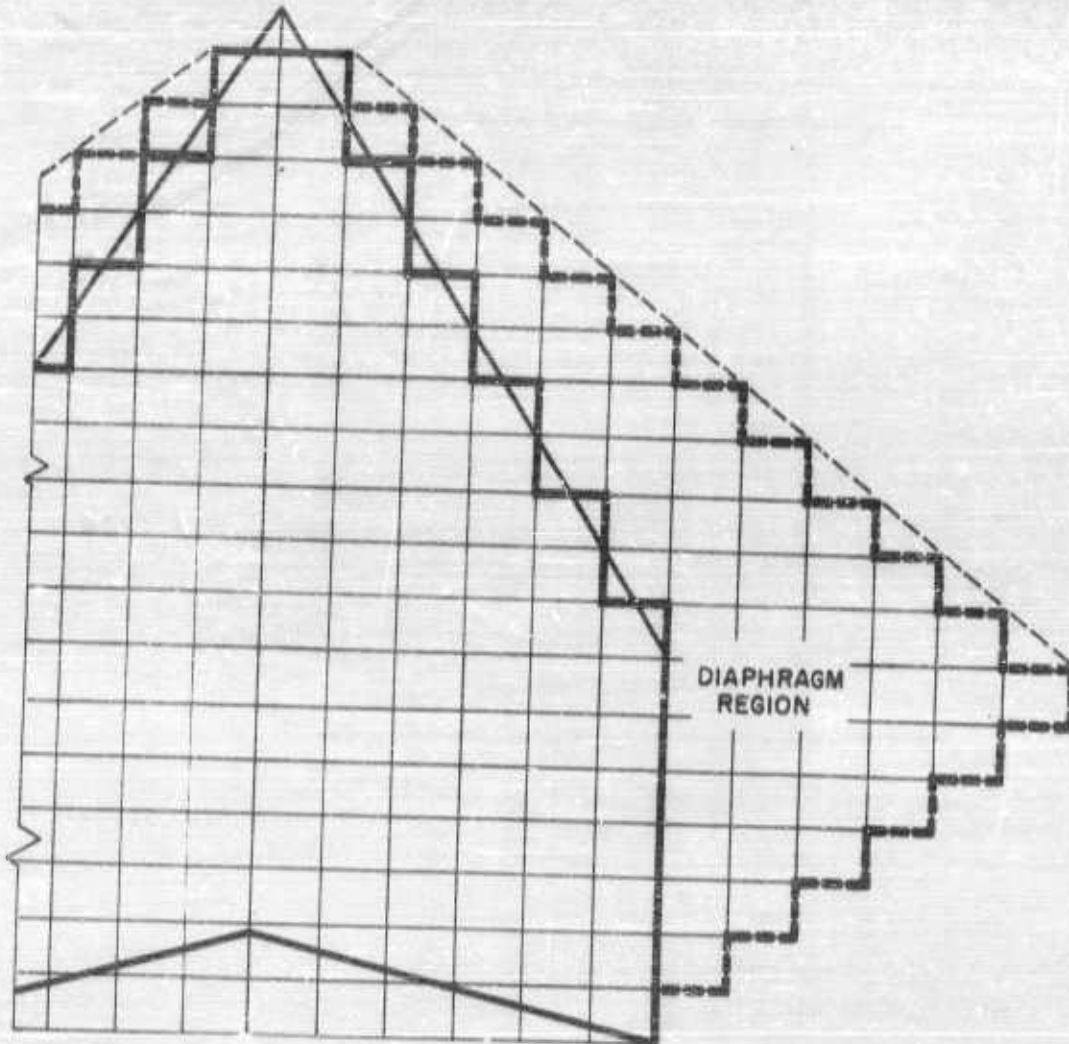


Fig. III.3 Positioning of the Mach Box Grid System on a Planform with Subsonic Leading Edges and Side Edges

**CONFIDENTIAL**

# CONFIDENTIAL

The foregoing rules were arrived at originally in connection with the PIC-method (Ref. 1). They were stated after giving due consideration to the following factors: (1) accuracy for the generalized forces, (2) the amount of computational labor. Needless to say, higher accuracy requires a larger amount of work. Therefore, for the final decision a compromise had to be made, i.e., one had to determine the point beyond which the improvement in accuracy is not sufficient to warrant the associated increases in the computations.

With the same number of boxes, experience has indicated that the VIC-method yields significantly better accuracy than the PIC-method. In view of this, one would think of reducing the minimum number of boxes set forth in Rule 1 from twelve to, say, eight. However, it is regarded as preferable to keep the minimum number of twelve for the following reason. For this class of planforms, the accuracies attainable for the generalized forces are, in general, poorer than those for purely supersonic planforms when the above rules are employed. By keeping the minimum number of boxes at twelve with the VIC-method, the computational precision is brought more in line with that for purely supersonic planforms.

## III.4 Planforms with Supersonic or Subsonic Leading Edges and Subsonic Trailing Edges

For planforms with subsonic trailing edges, the rules stated previously in Section III.3 apply in general with the following modifications to account for the diaphragm region behind the trailing edges (see Fig. III.4).

### Rules:

1. If the leading edge is supersonic, a minimum of twelve boxes along the midspan chord is to be used; if subsonic, sixteen boxes.
2. The diaphragm region behind the trailing edge must be composed of complete boxes only. Consequently the trailing edge is replaced by a jagged line (see Fig. III.4) and in this case partial boxes are not allowed.
3. For diaphragm regions associated with a subsonic leading edge or a side edge parallel to the flow, the condition of  $\Delta\psi = 0$  is equivalent to the condition of zero pressure difference. For the diaphragm boxes behind a subsonic trailing edge, the equivalence of these two alternative conditions is no longer true. Rather than setting  $\Delta\psi = 0$  for such diaphragm boxes, one must proceed in the following manner to satisfy the true boundary condition of  $\Delta\bar{p} = 0$ .

**CONFIDENTIAL**

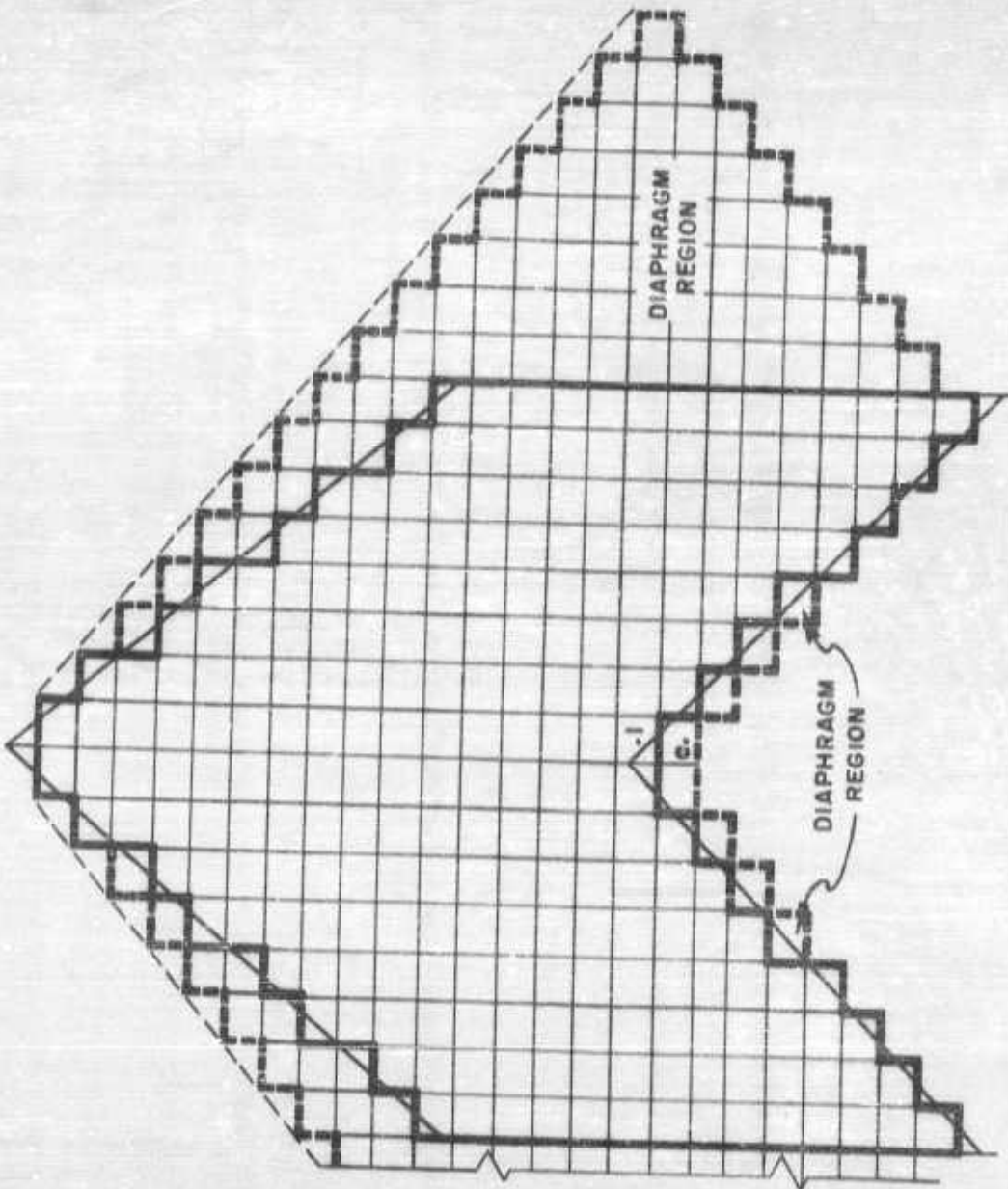


Fig. III. 4 Positioning of the Mach Box Grid System on a Planform with all Edges Subsonic

**CONFIDENTIAL**

# CONFIDENTIAL

Consider the center of box  $a$ . The value of  $\Delta\varphi$  at this point should be taken to be

$$(\Delta\varphi)_a = (\Delta\varphi)_t e^{-iA\left(\frac{x_a - x_t}{t}\right)} \quad \text{Eq. (3.2)}$$

where  $(\Delta\varphi)_t$  is the potential difference at the upstream trailing edge point  $t$  and  $(x_a - x_t)$  represents the distance between the center of box  $a$  and point  $t$ .\*

-----  
\*It should be noted that  $(\Delta\varphi)_t$  must be computed for the generalized force calculations (Appendix C), so that this necessary step does not add much to the complexity of the problem.

# CONFIDENTIAL

## SECTION IV

### DETERMINATION OF DOWNWASH DISTRIBUTION ON THE DIAPHRAGM REGION AND ITS EFFECT ON THE AIRLOAD DISTRIBUTION

Associated with any subsonic edge, there exists a disturbed region off the planform which influences the pressure distribution on the planform. Following Evvard's concept (Ref. 7), a thin impermeable diaphragm may be introduced in this region. This diaphragm is assumed to coincide with a stream sheet, and therefore it will not alter the flow. It can sustain no pressure difference at any point between its top and bottom surfaces. The latter condition allows the determination of the unknown vertical velocity (downwash) distribution on the diaphragm. The combination of the planform and the diaphragm forms a new surface which is purely supersonic and for which the downwash is known everywhere. The pressures (or the velocity potentials) may then be determined as for any other purely supersonic surface.

The illustrative examples shown below are carried out with the PIC-method. The VIC-method follows an identical procedure with these exceptions:

- (1) One must employ the VIC's  $(\Phi_{\mathcal{D},\mu} = \mathcal{R}_{\mathcal{D},\mu}^{(\psi)} + i \mathcal{J}_{\mathcal{D},\mu}^{(\psi)})$  instead of the PIC's  $(C_{\mathcal{D},\mu} = \mathcal{R}_{\mathcal{D},\mu} + i \mathcal{J}_{\mathcal{D},\mu})$ . Both of these quantities are defined in Appendix A.
- (2) For diaphragm regions near a subsonic leading edge or a side edge parallel to the flow, one must impose the boundary condition of  $\Delta\psi = 0$  at the centers of the boxes rather than  $\Delta\mathcal{F} = 0$ .
- (3) For the diaphragm behind a subsonic trailing edge, the true boundary condition of  $\Delta\mathcal{F} = 0$  dictates the use of the relation ( $x, y$  being behind the trailing edge)

$$\Delta\psi(x, y) = \Delta\psi(x_0(y), y) e^{-i\kappa \left(\frac{x-x_0}{\tau}\right)} ; \quad \text{Eq. (4.1)}$$

# CONFIDENTIAL

this expression is derived from the equation relating the pressure to the velocity potential

$$\Delta \bar{p} = \frac{\rho U}{\rho} \left\{ i k \Delta \bar{\psi} + t \frac{\partial(\Delta \bar{\psi})}{\partial x} \right\} \quad \text{Eq. (4.2)}$$

and the condition that  $\Delta \bar{p} = 0$  behind the trailing edge.

## IV.1 Determination of the Downwash Distribution on the Diaphragm Region

If the downwash over each diaphragm box is assumed constant the diaphragm region should be represented by those complete boxes of the grid system having their centers inside this region. Imposing the appropriate boundary condition at the centers of these boxes, the downwash distribution can be determined by "sequential solution" of the resultant equations. As an example, consider the rectangular wing shown in Fig. IV.1. For this case, the diaphragm boxes are (2,2), (3,2), (4,2) and (5,1).

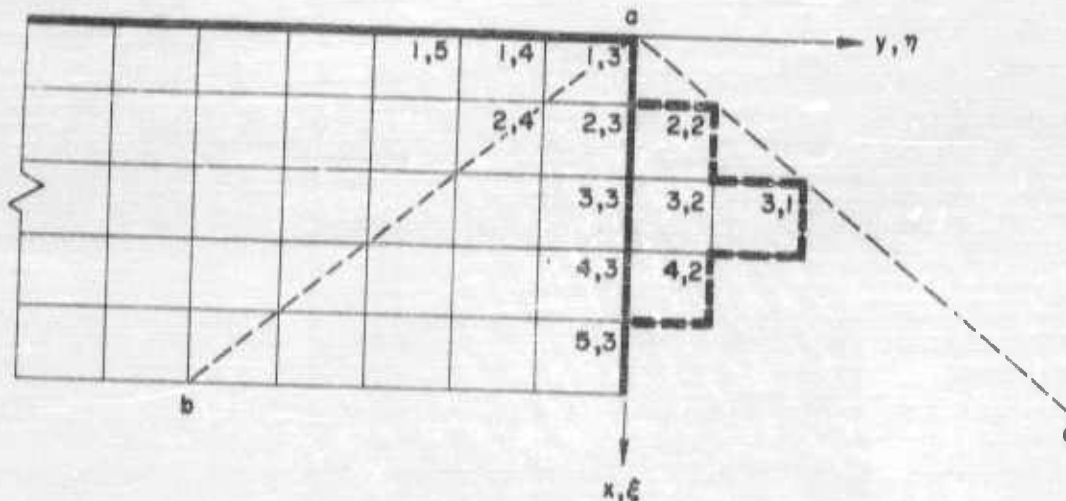


Fig. IV.1 Illustrative Example for the Treatment of the Side Edge

One has the following equations:

# CONFIDENTIAL

$$\bar{P}_{2,2} = 0 ; \bar{w}_{2,2} C_{0,0} + \bar{w}_{1,3} C_{6,1} = 0$$

$$\bar{P}_{3,1} = 0 ; \bar{w}_{3,1} C_{0,0} + \bar{w}_{2,2} C_{6,1} + \bar{w}_{1,3} C_{2,2} = 0$$

$$\bar{P}_{3,2} = 0 ; \bar{w}_{2,2} C_{0,0} + \bar{w}_{2,3} C_{1,1} + \bar{w}_{1,3} C_{2,1} + \bar{w}_{1,4} C_{2,2} + \bar{w}_{2,2} C_{1,0} = 0$$

$$\bar{P}_{4,2} = 0 ; \bar{w}_{2,2} C_{0,0} + \bar{w}_{3,3} C_{1,1} + \bar{w}_{2,4} C_{2,2} + \bar{w}_{1,5} C_{3,3} + \bar{w}_{2,2} C_{1,0} + \bar{w}_{2,3} C_{2,1} \\ + \bar{w}_{1,4} C_{3,2} + \bar{w}_{3,1} C_{1,1} + \bar{w}_{2,2} C_{2,0} + \bar{w}_{1,3} C_{2,1} = 0$$

Eqs. (4.3a-d)

It is noted that in each equation, there is only one unknown, provided all the preceding equations have been solved. This allows a simple sequential calculation and avoids the necessity of solving a simultaneous system. If a matrix formulation is used as in Ref. 8, there follows

$$\begin{bmatrix} C_{1,1} & 0 & 0 & 0 & 0 & 0 & | & C_{2,0} & 0 & 0 & 0 \\ C_{2,2} & 0 & 0 & 0 & 0 & 0 & | & C_{1,1} & C_{0,0} & 0 & 0 \\ C_{2,1} & C_{1,1} & C_{2,2} & 0 & 0 & 0 & | & C_{1,0} & 0 & C_{0,0} & 0 \\ C_{3,1} & C_{2,1} & C_{3,2} & C_{1,1} & C_{1,2} & C_{3,3} & | & C_{2,0} & C_{1,1} & C_{1,0} & C_{0,0} \end{bmatrix} \begin{bmatrix} \bar{w}_{1,3} \\ \bar{w}_{2,3} \\ \bar{w}_{1,4} \\ \bar{w}_{2,3} \\ \bar{w}_{2,4} \\ \bar{w}_{1,5} \\ \bar{w}_{2,2} \\ \bar{w}_{3,1} \\ \bar{w}_{3,2} \\ \bar{w}_{4,2} \end{bmatrix} = \begin{bmatrix} 0 \\ 0 \\ 0 \\ 0 \\ 0 \end{bmatrix}$$

Eq. (4.4)

or equivalently,

$$\begin{bmatrix} \bar{w}_{2,2} \\ \bar{w}_{3,1} \\ \bar{w}_{3,2} \\ \bar{w}_{4,2} \end{bmatrix} = - \begin{bmatrix} C_{0,0} & 0 & 0 & 0 \\ C_{1,1} & C_{2,0} & 0 & 0 \\ C_{1,0} & 0 & C_{0,0} & 0 \\ C_{2,0} & C_{1,1} & C_{1,0} & C_{0,0} \end{bmatrix}^{-1} \begin{bmatrix} C_{1,1} & 0 & 0 & 0 & 0 & 0 \\ C_{2,2} & 0 & 0 & 0 & 0 & 0 \\ C_{2,1} & C_{1,1} & C_{2,2} & 0 & 0 & 0 \\ C_{3,1} & C_{2,1} & C_{3,2} & C_{1,1} & C_{2,2} & C_{3,3} \end{bmatrix} \begin{bmatrix} \bar{w}_{1,3} \\ \bar{w}_{2,3} \\ \bar{w}_{1,4} \\ \bar{w}_{2,3} \\ \bar{w}_{2,4} \\ \bar{w}_{1,5} \end{bmatrix}$$

Eq. (4.5)

# CONFIDENTIAL

It is known from steady-state solutions that the downwash at the side edge, when approached from the diaphragm region, exhibits a square-root singularity and vanishes at the foremost Mach line. The assumption of constant downwash over each box of the diaphragm therefore introduces errors in the pressures over planform boxes near the side edge. If a large number of boxes is used, these discrepancies are confined to a small region near the tip, and the resultant accuracy for the total generalized forces is satisfactory. The process just described is the one suggested by Alternative 1, Section III.2.

To improve the airload estimation, especially when a small number of chordwise boxes is taken along the side edge, the effect of the singularity can be accounted for more accurately in the following manner.

Referring to Fig. IV.2, in Cartesian coordinates, the receiving point is  $(x, y)$  while  $\xi, \eta$  are running variables representing the influencing point. A characteristic coordinate system  $r, s$  with origin at  $(x, y)$  is defined such that the axes  $r$  and  $s$  are, respectively, the right and left forward Mach lines emanating from  $(x, y)$ . The new coordinates  $r$  and  $s$  are related to  $x, y, \xi$  and  $\eta$  through the equations

$$r = \frac{M}{2\beta} [(x-\xi) - \beta(y-\eta)]$$

$$s = \frac{M}{2\beta} [(x-\xi) + \beta(y-\eta)]$$

Eqs. (4.6a-b)

If the receiving point is on the side edge, i.e.,  $y=0$ , one may assume a downwash amplitude distribution

$$\bar{w}(r,s) = \frac{\bar{w}_s}{\sqrt{d}} \frac{r-r}{\sqrt{r-s}}$$

Eq. (4.7)

which exhibits the proper behavior at the side edge ( $r=s$  or  $y=0$ ) and vanishes on the foremost Mach line  $r=\eta$ . Here  $d$  is a typical length and  $\bar{w}_s$  is the "strength" of the downwash. For convenience,  $d$  will be taken as half the diagonal length of a Mach box.

It is more convenient to locate the origin of the coordinate system at the point for which the pressure or potential difference is to be determined. By coordinate transformation one obtains (see Figs. IV.3a-b)

**CONFIDENTIAL**

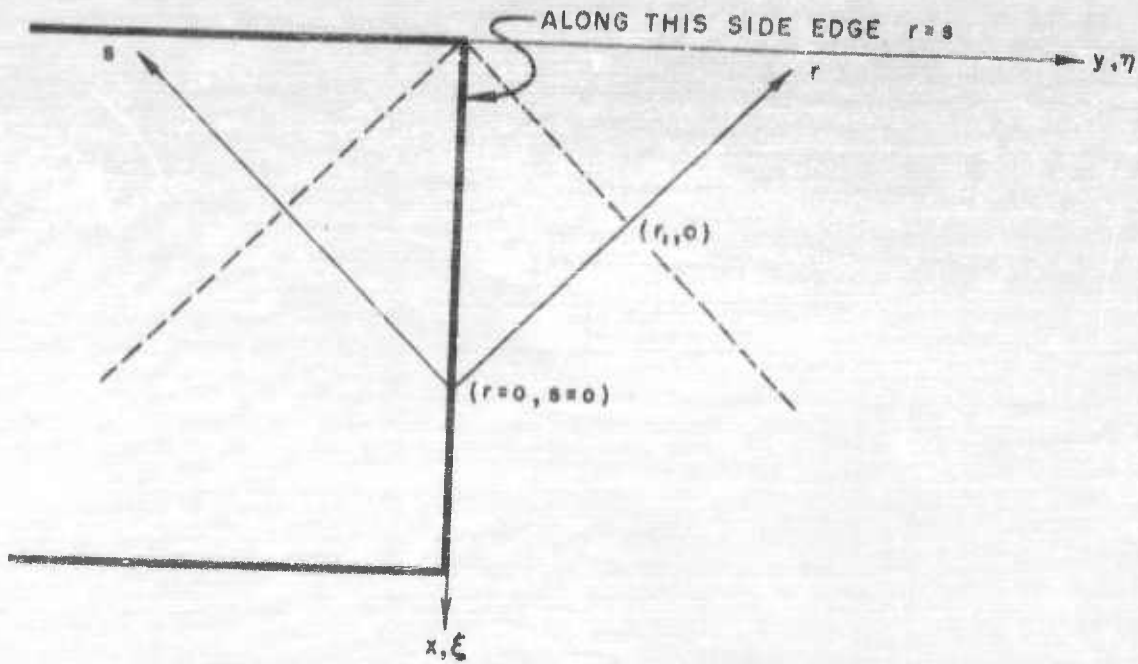


Fig. IV. 2 Characteristic Coordinate System

$$\bar{w}(r, s) = \frac{\bar{w}_s}{\sqrt{d}} \frac{r_1 - r}{\sqrt{r + s_0 - s}}$$

Eq. (4.8)

when the origin is on the diaphragm region, and

$$\bar{w}(r, s) = \frac{\bar{w}_s}{\sqrt{d}} \frac{r_1 - r}{\sqrt{r - r_0 - s}}$$

Eq. (4.9)

when the origin is on the platform.

It may be shown that for steady flow the pressure coefficients associated with these two cases are

**CONFIDENTIAL**

**CONFIDENTIAL**

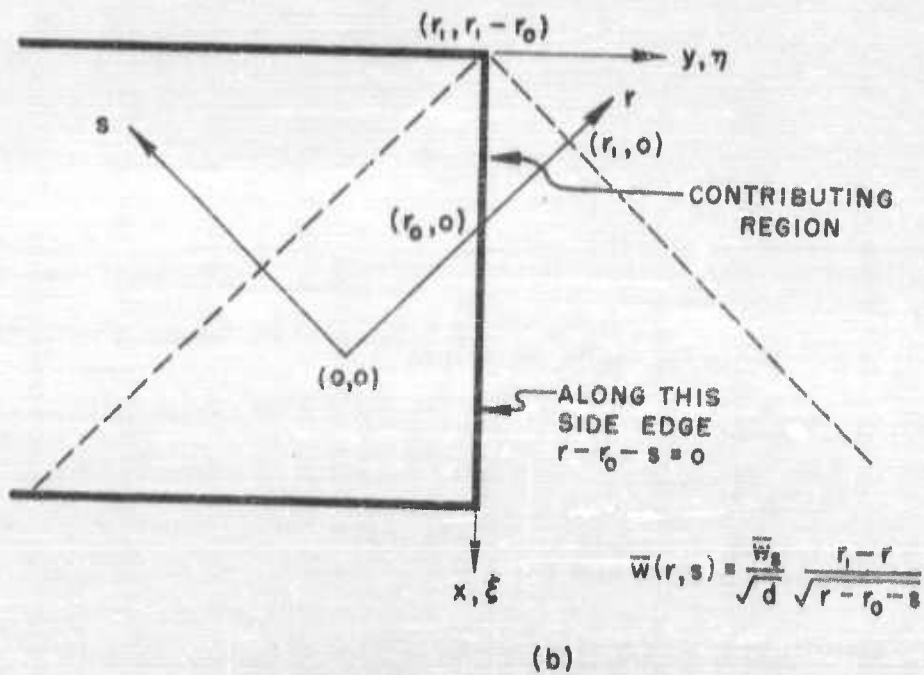
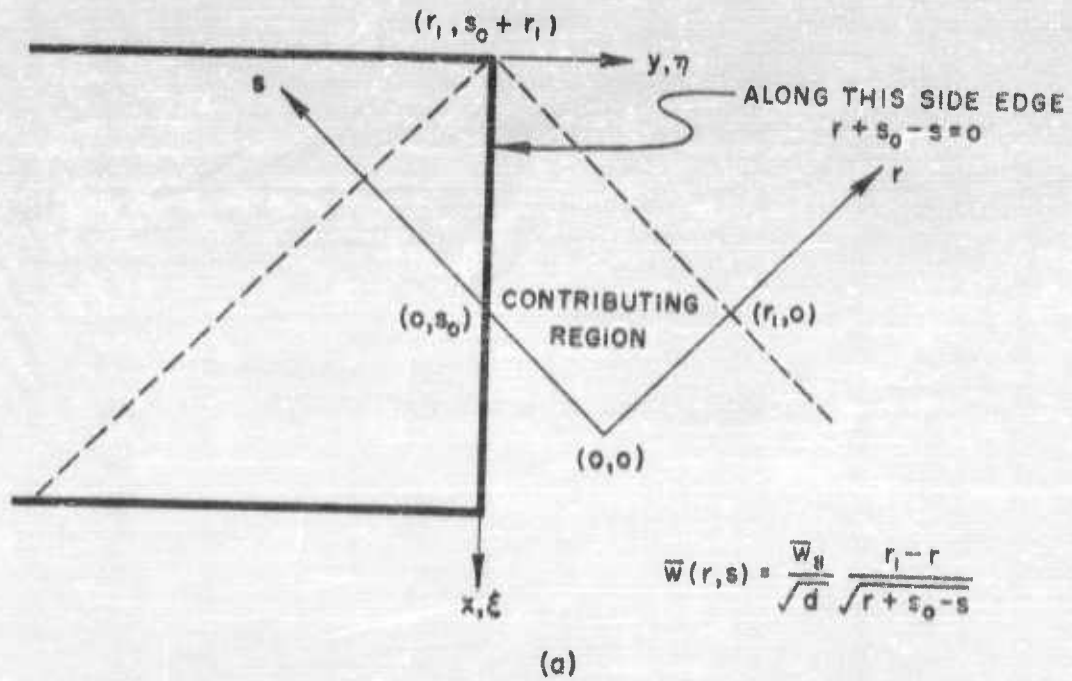


Fig. IV. 3 Singular Downwash Distribution Near a Side Edge

**CONFIDENTIAL**

# CONFIDENTIAL

$$C^{(s)} = \frac{h_u - h_l}{\left(\frac{\rho U \omega_s}{2}\right)} = -\sqrt{\frac{r_i}{d}} = C_a^{(s)} \text{ for Fig. IV.3a}$$

$$= -\sqrt{\frac{r_i}{d}} + \sqrt{\frac{r_o}{d}} = C_b^{(s)} \text{ for Fig. IV.3b}$$

Eqs. (4.10a-b)

Similarly, for the velocity potential coefficients, one has ( $t$ , being the streamwise dimension of a box)

$$\Phi^{(s)} = \frac{\varphi_u - \varphi_l}{\left(\frac{b, \omega_s}{\rho}\right)} = -\frac{4}{3} \left(\frac{r_i}{d}\right)^{3/2} = \Phi_a^{(s)} \text{ for Fig. IV.3a}$$

$$= -\frac{4}{3} \left(\frac{r_i}{d}\right)^{3/2} + 2 \left(\frac{r_i}{d}\right) \left(\frac{r_o}{d}\right)^{1/2} - \frac{2}{3} \left(\frac{r_o}{d}\right)^{3/2} = \Phi_b^{(s)} \text{ for Fig. IV.3b}$$

Eqs. (4.10c-d)

This refinement may be introduced in the Mach box scheme. To illustrate its application, consider the simple problem of a rectangular wing in steady flow at an angle of attack  $\alpha$ . The downwash at all points on the planform is  $U\alpha$ . Referring to Fig. IV.4, assume the following downwash distributions:

- (1) Singular distribution of strength  $w_{s1}$  over the region  $eac$ .
- (2) Additional singular distributions of strength  $w_{s2}$ ,  $w_{s3}$ ,  $w_{s4}$  over the regions  $efg$ ,  $ehj$ ,  $ehl$ , respectively.
- (3) Constant downwashes of strength  $w_{s1}$  and  $w_{s4}$  over boxes (3,1) and (4,1).

**CONFIDENTIAL**

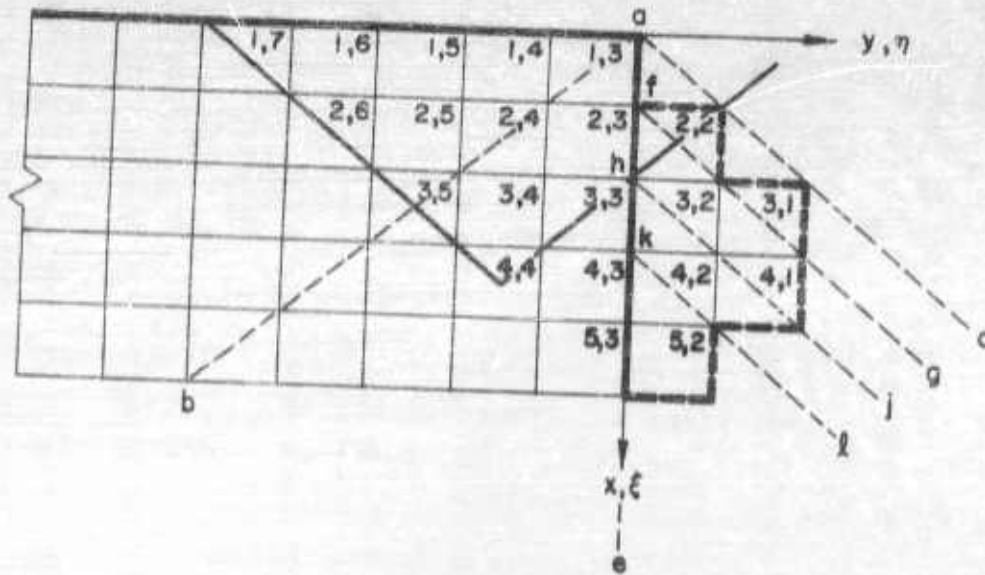


Fig. IV. 4 Illustrative Example for the Treatment of the Side Edge Including the Effect of Downwash Singularity

Satisfying the conditions of zero pressure at the centers of diaphragm boxes, one has

$$p_{2,2} = 0; \quad C_{1,1}(U_{\alpha}) + C_a^{(s)} \left( \frac{r_1}{d} - 1 \right) w_{s1} = 0$$

$$p_{3,1} = 0; \quad C_{2,2}(U_{\alpha}) + C_a^{(s)} \left( \frac{r_1}{d} - 1 \right) w_{s1} + C_{0,0} w_{s1} = 0$$

$$p_{3,2} = 0; \quad C_{2,2}(U_{\alpha}) + C_{1,1}(U_{\alpha}) + C_{2,1}(U_{\alpha}) + C_a^{(s)} \left( \frac{r_1}{d} - 2 \right) w_{s1} \\ + C_a^{(s)} \left( \frac{r_1}{d} - 1 \right) w_{s2} = 0$$

Eq. (4.11)

As in the previous example [Eqs. (4.5)], a sequential solution or a matrix solution of the above set of equations yields the desired downwashes on the diaphragm.

**CONFIDENTIAL**

# CONFIDENTIAL

## IV.2 Determination of the Pressure or Velocity Potential Distributions on the Platform

Once the downwash distribution in the diaphragm region is determined according to the previous section, the pressure or the velocity potential differences at the control points of the platform are next obtained. If the downwash over each diaphragm box is assumed constant, the procedure is identical with Appendix A [Eq. (A.6) or Eq. (A.8)], where only the pressure coefficients  $C_{p,i}$  or the potential coefficients  $\Phi_{i,\mu}$  associated with unit constant downwashes are involved. When the singularity in downwash is to be accounted for, the method is similar but additional tabulations for the coefficients  $C_a^{(s)}$ ,  $C_b^{(s)}$  (or  $\Phi_a^{(s)}$  and  $\Phi_b^{(s)}$ ) are necessary. For instance, the pressure at center of box (4,4) is (Fig. IV.4)

$$p_{4,4} = \frac{2\rho U}{\beta} \left[ U_d (C_{0,0} + C_{1,1} + C_{2,2} + C_{3,3} + C_{4,0} + C_{2,0} + C_{3,0} + C_{2,1} + C_{3,2} + C_{4,1} + C_{2,1} + C_{3,1} + C_{3,1}) + w_{s1} C_b^{(s)} \left( \frac{r_1}{d} = 5, \frac{r_2}{d} = 3 \right) + w_{s2} C_b^{(s)} \left( \frac{r_1}{d} = 4, \frac{r_2}{d} = 3 \right) \right]$$

Eq. (4.12)

## IV.3 Aerodynamic Influence Coefficients Associated with Singular Downwash Distributions

The general expressions for the coefficients  $C_a^{(s)}$ ,  $C_b^{(s)}$ ,  $\Phi_a^{(s)}$  and  $\Phi_b^{(s)}$  are as follows:

$$C_a^{(s)} = -8i\epsilon \frac{\beta^2}{M^2} \sqrt{\frac{r_1}{d}} \left\{ \bar{I}_0(\epsilon, \sigma) - \bar{I}_1(\epsilon, \sigma) \right\} - 2\sqrt{\frac{r_1}{d}} \bar{I}_0(\epsilon, \sigma) = \frac{p_0 - p_\infty}{\left( \frac{2\rho U d_5}{\beta} \right)}$$

$$C_b^{(s)} = -8i\epsilon \frac{\beta^2}{M^2} \sqrt{\frac{r_1}{d}} \left\{ \bar{P}_0(\epsilon, \bar{\sigma}) - \bar{P}_1(\epsilon, \bar{\sigma}) \right\} - 2\sqrt{\frac{r_1}{d}} \bar{P}_0(\epsilon, \bar{\sigma}) = \frac{p_0 - p_\infty}{\left( \frac{2\rho U d_5}{\beta} \right)}$$

Eqs. (4.13a-b)

# CONFIDENTIAL

$$\Phi_a^{(s)} = -4 \left(\frac{r_i}{d}\right)^{3/2} \left\{ \bar{I}_0(\epsilon, \sigma) - \bar{I}_1(\epsilon, \sigma) \right\} = \frac{\bar{y}_U - \bar{y}_L}{\left(\frac{b_i \bar{u}_s}{\beta}\right)}$$

$$\Phi_t^{(s)} = -4 \left(\frac{r_i}{d}\right)^{3/2} \left\{ \bar{P}_0(\epsilon, \bar{\sigma}) - \bar{P}_1(\epsilon, \bar{\sigma}) \right\} = \frac{\bar{y}_U - \bar{y}_L}{\left(\frac{b_i \bar{u}_s}{\beta}\right)}$$

Eqs. (4.13c-d)

where

$\omega$  is the circular frequency;

$d$  is a typical length taken to be half the diagonal length of the Mach box;

$r_0, r_i, s_0$  are lengths along the characteristic axes as shown in Fig. IV.3;

$$\epsilon = \frac{r_i}{2} \left(\frac{\omega M}{U\beta}\right) = \frac{1}{4} \left(\frac{r_i}{d}\right) \bar{A}_i$$

$$\sigma = \frac{s_0}{r_i}$$

$$\bar{\sigma} = \frac{r_0}{r_i}$$

and

$$\bar{I}_n(\epsilon, \sigma) = \frac{1}{4\pi r_i^{n+1/2}} \int_0^{r_i} \int_0^{s_0+r} \frac{r^n}{\sqrt{r+s_0-s}} \frac{1}{\sqrt{rs}} e^{-i\frac{\omega M}{U\beta}(r+s)} \cos\left(\frac{2\omega}{U\beta}\sqrt{rs}\right) ds dr$$

$$\bar{P}_n(\epsilon, \bar{\sigma}) = \frac{1}{4\pi r_i^{n+1/2}} \int_{r_0}^{r_i} \int_0^{r-r_0} \frac{r^n}{\sqrt{r-r_0-s}} \frac{1}{\sqrt{rs}} e^{-i\frac{\omega M}{U\beta}(r+s)} \cos\left(\frac{2\omega}{U\beta}\sqrt{rs}\right) ds dr$$

Eqs. (4.14a-b)

# CONFIDENTIAL

For the steady case, Eqs. (4.13a-d) reduce to the simple forms of Eqs. (4.10a-d). In general, however, the integrations for  $\bar{I}_n$  and  $\bar{P}_n$  must be carried out numerically. When computing  $\Phi^{(s)}$ , one need not tabulate  $\bar{I}_0$  and  $\bar{I}_1$  (or  $\bar{P}_0$  and  $\bar{P}_1$ ) independently as in the case of  $C^{(s)}$ . By suitable transformations of variables, the double integrals reduce to the single integrals

$$\begin{aligned} \bar{I}_n(\epsilon, \sigma) = & e^{-i\epsilon\sigma} \int_0^1 z^{2n} e^{-3i\epsilon z^2} \left\{ \frac{1}{z} J_0\left(\frac{4\epsilon}{M} z \sqrt{z^2 + \sigma}\right) J_0(\epsilon[z^2 + \sigma]) \right. \\ & + \sum_{m=1}^{\infty} (-1)^m J_{4m}\left(\frac{4\epsilon}{M} z \sqrt{z^2 + \sigma}\right) J_{2m}(\epsilon[z^2 + \sigma]) \\ & \left. + i \sum_{m=0}^{\infty} (-1)^m J_{4m+2}\left(\frac{4\epsilon}{M} z \sqrt{z^2 + \sigma}\right) J_{2m+1}(\epsilon[z^2 + \sigma]) \right\} dz \end{aligned}$$

$$\begin{aligned} \bar{P}_n(\epsilon, \bar{\sigma}) = & e^{i\epsilon\bar{\sigma}} \int_{\sqrt{\bar{\sigma}}}^1 z^{2n} e^{-3i\epsilon z^2} \left\{ \frac{1}{z} J_0\left(\frac{4\epsilon}{M} z \sqrt{z^2 - \bar{\sigma}}\right) J_0(\epsilon[z^2 - \bar{\sigma}]) \right. \\ & + \sum_{m=1}^{\infty} (-1)^m J_{4m}\left(\frac{4\epsilon}{M} z \sqrt{z^2 - \bar{\sigma}}\right) J_{2m}(\epsilon[z^2 - \bar{\sigma}]) \\ & \left. + i \sum_{m=0}^{\infty} (-1)^m J_{4m+2}\left(\frac{4\epsilon}{M} z \sqrt{z^2 - \bar{\sigma}}\right) J_{2m+1}(\epsilon[z^2 - \bar{\sigma}]) \right\} dz \end{aligned}$$

Eqs. (4.15a-b)

where  $J_p$  is the Bessel function of the first kind of order  $p$ . The infinite series in the integrands are rapidly convergent for the ranges of Mach number and reduced frequency of interest, and only a few terms need be retained. It is worth noting that the integrands are functions of  $z^2$ ,  $\sigma$  is an integer or a fraction of integers and  $\bar{\sigma}$  is a fraction of integers and less than 1.

The numerical method suggested here is a modification of Gauss' quadrature. It can be proved that the integration formula

# CONFIDENTIAL

$$\int_0^1 f(z^2) dz = \sum_{j=1}^N H_j f(z_j^2)$$

Eq. (4.16)

is exact if  $f(z^2)$  is a polynomial of degree  $(2N-1)$  or less in  $z^2$ , provided the  $z_j^2$  are chosen properly.  $H_j$ 's are the weighting factors associated with this set of  $z_j^2$  (see Ref. 1). For  $N=5$ , one obtains

$z_1^2 = 0.022,163,567$	$H_1 = 0.295,524,215$
$z_2^2 = 0.187,831,574$	$H_2 = 0.269,266,739$
$z_3^2 = 0.461,597,344$	$H_3 = 0.219,086,348$
$z_4^2 = 0.748,334,658$	$H_4 = 0.149,451,361$
$z_5^2 = 0.948,493,910$	$H_5 = 0.066,671,338$

Eqs. (4.17)

For low to moderate frequencies, the integrand of  $I_n$  can be satisfactorily represented by the polynomial

$$f(z^2) = a_0 + a_1 z^2 + a_2 z^4 + \dots + a_n z^{2n}$$

which passes through points  $z_1, \dots, z_5$ ; and the integration for  $I_n$  according to Eq. (4.16) will be adequate.

For  $\bar{P}_n$ , the situation is somewhat different since the range of integration varies with  $\bar{\sigma}$ . However, it has been found by some trial calculations that Eq. (4.16) can still be used with the following modification:

$$\begin{aligned} \bar{P}_n &= e^{ic\bar{\sigma}} \int_0^1 z^{2n} e^{-sicz^2} \{Q(z^2)\} dz \\ &= e^{ic\bar{\sigma}} \left[ \int_0^{\sqrt{\bar{\sigma}}} z^{2n} e^{-sicz^2} \{Q(z^2)\} dz - \frac{1}{2} \bar{\sigma}^{n+\frac{1}{2}} \int_0^1 z^{2n} e^{-sic\bar{\sigma}z^2} dz \right] \end{aligned} \quad \text{Eq. (4.18)}$$

where  $Q(z^2)$  is defined to be

# CONFIDENTIAL

$$\begin{aligned}
 Q(z^2) &= \left\{ \frac{1}{2} J_0 \left( \frac{4\epsilon}{M} z \sqrt{z^2 - \bar{\sigma}} \right) J_0(\epsilon[z^2 - \bar{\sigma}]) \right. \\
 &\quad + \sum_{m=1}^{\infty} (-1)^m J_{4m} \left( \frac{4\epsilon}{M} z \sqrt{z^2 - \bar{\sigma}} \right) J_{2m}(\epsilon[z^2 - \bar{\sigma}]) \\
 &\quad \left. + i \sum_{m=0}^{\infty} (-1)^m J_{4m+2} \left( \frac{4\epsilon}{M} z \sqrt{z^2 - \bar{\sigma}} \right) J_{2m+1}(\epsilon[z^2 - \bar{\sigma}]) \right\} \quad \text{when } z^2 \gg \bar{\sigma} \\
 &= \frac{1}{2} \quad \text{when } z^2 \leq \bar{\sigma}
 \end{aligned}$$

Eq. (4.19)

By numerical integration  $\bar{P}_n$  becomes:

$$\bar{P}_n(\epsilon, \bar{\sigma}) \approx e^{i\epsilon\bar{\sigma}} \sum_{j=1}^N H_j \left\{ z_j^{2n-3i\epsilon z_j^2} Q(z_j^2) - \frac{1}{2} \bar{\sigma}^{n+\frac{1}{2}} z_j^{2n-3i\epsilon\bar{\sigma} z_j^2} \right\} \quad \text{Eq. (4.20)}$$

For higher frequencies, the integrand becomes sinuous and a higher-degree polynomial must be considered. Reference 1 discusses this situation, and outlines the steps in devising a nine-point integration ( $N=9$ ) formula which must be used, especially for the  $\bar{P}_n$ -coefficients, when the frequencies are relatively high.

# CONFIDENTIAL

## BIBLIOGRAPHY

1. Zartarian, G. and Hsu, P. T., Theoretical Studies on the Prediction of Unsteady Supersonic Airloads on Elastic Wings. Part I - Investigations on the Use of Oscillatory Supersonic Aerodynamic Influence Coefficients. WADC Technical Report 56-97, Part I, December 1955. (Confidential - Title Unclassified).
2. Harvard Computation Laboratory, Staff of, Tables of Oscillatory Supersonic Aerodynamic Influence Coefficients (AF Problem 101). Progress Report No. 39, Design and Operation of Digital Computing Machinery, Contract AF33(616)-2717, May 1955 (to be published as WADC Technical Report 54-113).
3. Zartarian, G., Heller, A., and Ashley, H., Application of Piston Theory to Certain Elementary Aeroelastic Problems. Proceedings of the Midwestern Conference on Fluid Mechanics, Purdue University, West Lafayette, Indiana, September 1955.
4. Landahl, M., Mollé-Christensen, E., and Ashley, H., Parametric Studies of Viscous and Nonviscous Unsteady Flows. OSR Technical Report No. 55-13, M.I.T. Fluid Dynamics Research Group Report No. 55-1, April 1955.
5. Pines, S., Liban, E., Neuringer, J., and Rabinowitz, S., Flutter Analysis of an Elastic Wing with Supersonic Edges. Republic Aviation Corporation Report E-SAF-1, April 1953.
6. Pines, S., and Dugundji, J., Aerodynamic Flutter Derivatives of a Flexible Wing with Supersonic Edges. Aircraft Industries Association Report Number ARTC-7, February 1954.
7. Evvard, J. C., Use of Source Distribution for Evaluating Theoretical Aerodynamics of Thin Finite Wings at Supersonic Speeds. NACA Report 951, 1950.
8. Pines, S., and Dugundji, J., Application of Aerodynamic Flutter Derivatives to Flexible Wings with Supersonic and Subsonic Edges. Republic Aviation Corporation Report E-SAF-2, April 1954.
9. Garrick, I.E., and Rubinow, S. I., Flutter and Oscillating Air-Force Calculations for an Airfoil in a Two-Dimensional Supersonic Flow. NACA Report 846, 1946.

# CONFIDENTIAL

## BIBLIOGRAPHY (Cont'd.)

10. National Bureau of Standards, Tables of Chebyshev Polynomials  $S_n(x)$  and  $C_n(x)$ . Applied Mathematics Series 9, United States Government Printing Office, Washington, 1952.
11. Crout, P. D., An Application of Polynomial Approximation to the Solution of Integral Equations Arising in Physical Problems, Journal of Mathematics and Physics, Vol. XIX, No. 1, January 1940.
12. Smilg, B., and Wasserman, L. S., Application of Three-Dimensional Flutter Theory to Aircraft Structures. AF Technical Report 4798, July 1942.
13. Voss, H. M., Zartarian, G., and Hsu, P. T., Application of Numerical Integration Techniques to the Low-Aspect-Ratio Flutter Problem in Subsonic and Supersonic Flows. M.I.T. Aeroelastic and Structures Research Laboratory Technical Report 52-3, Contract No. NOn(s) 53-564-c for Bureau of Aeronautics, USN, October 1954.
14. Siddall, J., and Isakson, G., Approximate Analytical Methods for Determining Natural Modes and Frequencies of Vibration. M.I.T. Aeroelastic and Structures Research Laboratory, Contract No. N5ori-07833, ONR Project NR-035-259, January 1951.
15. Huckel, V., Tabulation of the  $f_n$ -Functions which Occur in the Aerodynamic Theory of Oscillatory Wings in Supersonic Flow. NACA Technical Note 3606, February 1956.

# CONFIDENTIAL

## APPENDIX A

### PRESSURE AND VELOCITY POTENTIAL CALCULATIONS

#### A.1 Pressure Influence Coefficients for Square Boxes

Although the present report concentrates on applications of the Mach box scheme, influence coefficient formulas are listed first for the square boxes, since extensive tables of these coefficients already exist. The pressure difference  $p_{n,m}^{v,\mu}$  at the center of the receiving box  $(n,m)$  due to a constant downwash  $\bar{w}_{v,\mu} e^{i\omega t}$  at the sending box  $(v,\mu)$  is (Fig. A.1).

$$p_{n,m}^{v,\mu} = 2\sigma Ue^{i\omega t} \bar{w}_{v,\mu} (\bar{R}_{\bar{v},\bar{\mu}} + i\bar{I}_{\bar{v},\bar{\mu}}) \quad \text{Eq. (A.1)}$$

where  $\bar{v} = n - v$ ,  $\bar{\mu} = m - \mu$  and  $\bar{R} + i\bar{I}$  is the associated pressure influence coefficient. As depicted in the figure, the integers  $n$  and  $m$  indicate that to reach the receiving box one moves  $n$  boxes downstream and  $m$  boxes to the right from some arbitrarily designated reference box  $(0,0)$ . Similarly  $\bar{v}$  and  $\bar{\mu}$  represent the number of steps downstream and to the right, respectively, that one moves in going from the sending box to the receiving box. In supersonic flow  $\bar{v} > 0$  always.

The total pressure at the center of  $(n,m)$  is therefore

$$p_{n,m} = \sum_{v,\mu} p_{n,m}^{v,\mu} = 2\sigma Ue^{i\omega t} \sum_{v,\mu} \bar{w}_{v,\mu} (\bar{R}_{\bar{v},\bar{\mu}} + i\bar{I}_{\bar{v},\bar{\mu}}) \quad \text{Eq. (A.2)}$$

where the summation extends over all boxes  $(v,\mu)$  that lie partially or totally inside the forward Mach cone emanating from the center of box  $(n,m)$ . These coefficients are tabulated in Ref. 2. Only positive values of  $\bar{\mu}$  need be considered since by symmetry,

$$\bar{R}_{\bar{v},-\bar{\mu}} + i\bar{I}_{\bar{v},-\bar{\mu}} = \bar{R}_{\bar{v},\bar{\mu}} + i\bar{I}_{\bar{v},\bar{\mu}} \quad \text{Eq. (A.3)}$$

A slight error appears in Eq. (7a) of Ref. 2, and is carried through in the tables. The correct expression should read

**CONFIDENTIAL**

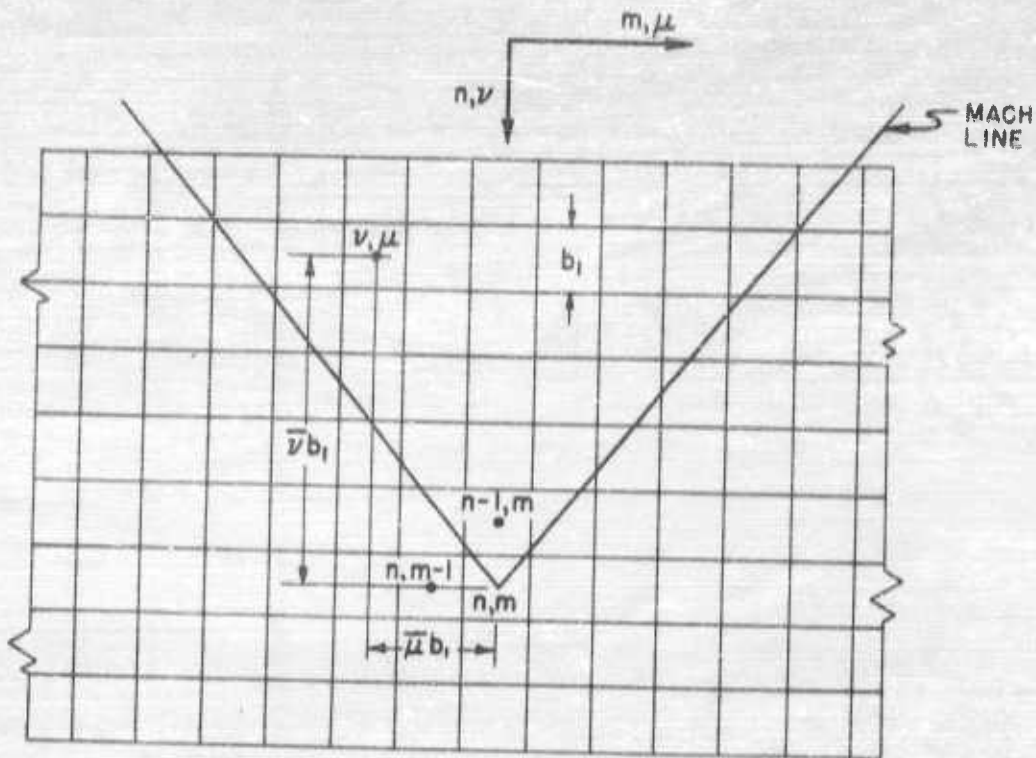


Fig. A.1 Square Grid System

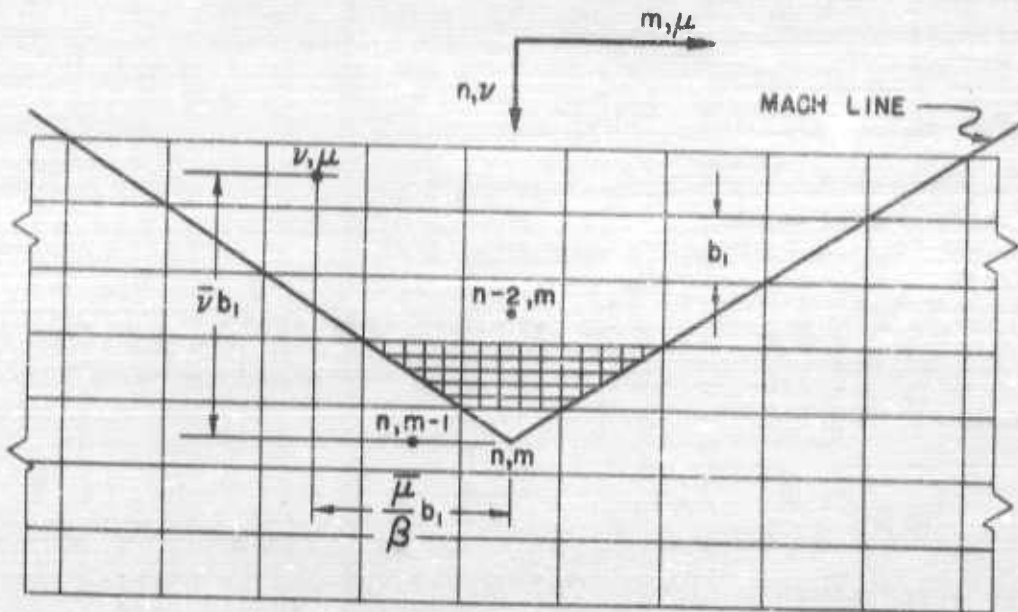


Fig. A.2 Mach Grid System

**CONFIDENTIAL**

# CONFIDENTIAL

$$\bar{R}_0 = \frac{1}{\beta} \left[ -1 + \frac{27}{400} \left( \frac{\bar{k}_1}{M} \right)^2 - \frac{27(4M^2+3)}{128,000} \left( \frac{\bar{k}_1}{M} \right)^4 \right] \quad \text{Eq. (A.4)}$$

Furthermore, the accuracy of  $\bar{R}_{0,0}$  in the most extreme cases (i.e., large  $k_1$  at low Mach numbers) is no better than five units in the third decimal place. For these high frequencies and low Mach numbers, this is not serious, since it is known that the accuracies for the rows  $\bar{v} > 2$  are much poorer.

## A.2 Aerodynamic Influence Coefficients for Mach Boxes

For Mach boxes, the pressure difference at the center of the receiving point  $(n,m)$  due to a constant downwash  $\bar{w}_{\nu,\mu} e^{i\omega t}$  at the sending box  $(\nu,\mu)$  is defined as follows (Fig. A.2):

$$p_{n,m}^{\nu,\mu} = \frac{2\rho U}{\beta} e^{i\omega t} \bar{w}_{\nu,\mu} (\mathcal{R}_{\nu,\mu} + i\mathcal{J}_{\nu,\mu}) \quad \text{Eq. (A.5)}$$

This definition is more convenient for tabulations, and for the steady case  $\mathcal{R}_{\nu,\mu}$  is independent of Mach number. Accordingly, the total pressure at the center of  $(n,m)$  is

$$p_{n,m} = \sum_{\nu,\mu} p_{n,m}^{\nu,\mu} = \frac{2\rho U}{\beta} e^{i\omega t} \sum_{\nu,\mu} \bar{w}_{\nu,\mu} (\mathcal{R}_{\nu,\mu} + i\mathcal{J}_{\nu,\mu}) \quad \text{Eq. (A.6)}$$

The velocity potential difference at  $(n,m)$  due to a constant downwash  $\bar{w}_{\nu,\mu} e^{i\omega t}$  at the sending box is

$$\Delta\varphi_{n,m}^{\nu,\mu} = \frac{b_1}{\beta} e^{i\omega t} \bar{w}_{\nu,\mu} (\mathcal{R}_{\nu,\mu}^{(\varphi)} + i\mathcal{J}_{\nu,\mu}^{(\varphi)}) \quad \text{Eq. (A.7)}$$

The total velocity potential difference at  $(n,m)$  is

$$\Delta\varphi_{n,m} = \sum_{\nu,\mu} \Delta\varphi_{n,m}^{\nu,\mu} = \frac{b_1}{\beta} e^{i\omega t} \sum_{\nu,\mu} \bar{w}_{\nu,\mu} (\mathcal{R}_{\nu,\mu}^{(\varphi)} + i\mathcal{J}_{\nu,\mu}^{(\varphi)}) \quad \text{Eq. (A.8)}$$

Again by symmetry,

# CONFIDENTIAL

$$R_{\bar{v}, -\bar{\mu}} + i J_{\bar{v}, -\bar{\mu}} = R_{\bar{v}, \bar{\mu}} + i J_{\bar{v}, \bar{\mu}}$$

$$R_{\bar{v}, -\bar{\mu}}^{(\varphi)} + i J_{\bar{v}, -\bar{\mu}}^{(\varphi)} = R_{\bar{v}, \bar{\mu}}^{(\varphi)} + i J_{\bar{v}, \bar{\mu}}^{(\varphi)}$$

Eqs. (A.9a-b)

## a. Exact Expressions

The exact expressions for the PIC's and the VIC's are now given. These were derived by using the series expansion for the velocity potential given by Watkins of NACA (no formal reference available, see Ref. 1).

$$R_{0,0} + i J_{0,0} = -e^{-i\frac{\bar{k}_1}{2}} J_0\left(\frac{\bar{k}_1}{2M}\right) - \frac{i\bar{k}_1}{2} \frac{\beta^2}{M^2} f_0\left(M, \frac{\bar{k}_1}{2}\right), \quad \bar{v} = \bar{\mu} = 0$$

$$R_{\bar{v}, \bar{v}} + i J_{\bar{v}, \bar{v}} = +\frac{1}{\pi} e^{-i\bar{k}_1(\bar{v}+\frac{1}{2})} \left[ J_0\left(\frac{\bar{k}_1}{M}[\bar{v}+\frac{1}{2}]\right) \left(\sin^{-1} \frac{2\bar{v}-1}{2\bar{v}+1} - \frac{\pi}{2}\right) + \sum_{r=1}^{\infty} \frac{(-1)^r}{r} J_{2r}\left(\frac{\bar{k}_1}{M}[\bar{v}+\frac{1}{2}]\right) \sin\left(2r \sin^{-1} \frac{2\bar{v}-1}{2\bar{v}+1}\right) \right] \\ + \frac{i\bar{k}_1}{\pi} \frac{\beta^2}{M^2} \int_{\bar{v}-\frac{1}{2}}^{\bar{v}+\frac{1}{2}} e^{-i\bar{k}_1 X} \left[ J_0\left(\frac{\bar{k}_1}{M} X\right) \left(\sin^{-1} \frac{2\bar{v}-1}{2X} - \frac{\pi}{2}\right) + \sum_{r=1}^{\infty} \frac{(-1)^r}{r} J_{2r}\left(\frac{\bar{k}_1}{M} X\right) \sin\left(2r \sin^{-1} \frac{2\bar{v}-1}{2X}\right) \right] dX, \\ \bar{v} = \bar{\mu} \geq 1$$

$$R_{\bar{v}, 0} + i J_{\bar{v}, 0} = -\frac{2}{\pi} e^{-i\bar{k}_1(\bar{v}+\frac{1}{2})} \left[ J_0\left(\frac{\bar{k}_1}{M}[\bar{v}+\frac{1}{2}]\right) \sin^{-1} \frac{1}{2\bar{v}+1} + \sum_{r=1}^{\infty} \frac{(-1)^r}{r} J_{2r}\left(\frac{\bar{k}_1}{M}[\bar{v}+\frac{1}{2}]\right) \sin\left(2r \sin^{-1} \frac{1}{2\bar{v}+1}\right) \right] \\ + \frac{2}{\pi} e^{-i\bar{k}_1(\bar{v}-\frac{1}{2})} \left[ J_0\left(\frac{\bar{k}_1}{M}[\bar{v}-\frac{1}{2}]\right) \sin^{-1} \frac{1}{2\bar{v}-1} + \sum_{r=1}^{\infty} \frac{(-1)^r}{r} J_{2r}\left(\frac{\bar{k}_1}{M}[\bar{v}-\frac{1}{2}]\right) \sin\left(2r \sin^{-1} \frac{1}{2\bar{v}-1}\right) \right] \\ - \frac{2i\bar{k}_1}{\pi} \frac{\beta^2}{M^2} \int_{\bar{v}-\frac{1}{2}}^{\bar{v}+\frac{1}{2}} e^{-i\bar{k}_1 X} \left[ J_0\left(\frac{\bar{k}_1}{M} X\right) \sin^{-1} \frac{1}{2X} + \sum_{r=1}^{\infty} \frac{(-1)^r}{r} J_{2r}\left(\frac{\bar{k}_1}{M} X\right) \sin\left(2r \sin^{-1} \frac{1}{2X}\right) \right] dX, \\ \bar{v} \geq 1 \\ \bar{\mu} = 0$$

# CONFIDENTIAL

$$\begin{aligned}
 R_{\bar{\nu}, \bar{\mu}} + i \int_{\bar{\nu}, \bar{\mu}} = \frac{1}{\pi} & e^{-i\bar{k}_1(\bar{\nu} + \frac{1}{2})} \left[ J_0 \left( \frac{\bar{k}_1}{M} [\bar{\nu} + \frac{1}{2}] \right) \left( \sin^{-1} \frac{2\bar{\mu}-1}{2\bar{\nu}+1} - \sin^{-1} \frac{2\bar{\mu}+1}{2\bar{\nu}+1} \right) \right. \\
 & + \sum_{r=1}^{\infty} \frac{(-1)^r}{r} J_{2r} \left( \frac{\bar{k}_1}{M} [\bar{\nu} + \frac{1}{2}] \right) \left\{ \sin(2r \sin^{-1} \frac{2\bar{\mu}-1}{2\bar{\nu}+1}) - \sin(2r \sin^{-1} \frac{2\bar{\mu}+1}{2\bar{\nu}+1}) \right\} \\
 & - \frac{1}{\pi} e^{-i\bar{k}_1(\bar{\nu} - \frac{1}{2})} \left[ J_0 \left( \frac{\bar{k}_1}{M} [\bar{\nu} - \frac{1}{2}] \right) \left( \sin^{-1} \frac{2\bar{\mu}-1}{2\bar{\nu}-1} - \sin^{-1} \frac{2\bar{\mu}+1}{2\bar{\nu}-1} \right) \right. \\
 & + \sum_{r=1}^{\infty} \frac{(-1)^r}{r} J_{2r} \left( \frac{\bar{k}_1}{M} [\bar{\nu} - \frac{1}{2}] \right) \left\{ \sin(2r \sin^{-1} \frac{2\bar{\mu}-1}{2\bar{\nu}-1}) - \sin(2r \sin^{-1} \frac{2\bar{\mu}+1}{2\bar{\nu}-1}) \right\} \\
 & + \frac{i\bar{k}_1 \bar{\mu}^2}{\pi M^2} \int_{\bar{\nu}-\frac{1}{2}}^{\bar{\nu}+\frac{1}{2}} e^{-i\bar{k}_1 X} \left[ J_0 \left( \frac{\bar{k}_1}{M} X \right) \left( \sin^{-1} \frac{2\bar{\mu}-1}{2X} - \sin^{-1} \frac{2\bar{\mu}+1}{2X} \right) + \sum_{r=1}^{\infty} \frac{(-1)^r}{r} J_{2r} \left( \frac{\bar{k}_1}{M} X \right) \left\{ \sin(2r \sin^{-1} \frac{2\bar{\mu}-1}{2X}) - \sin(2r \sin^{-1} \frac{2\bar{\mu}+1}{2X}) \right\} \right] dX,
 \end{aligned}$$

$$\bar{\nu} > \bar{\mu} \geq 1$$

Eqs. (A.10a-d)

$$R_{0,0}^{(0)} + i \int_{0,0}^{(0)} = -f_0 \left( M, \frac{\bar{k}_1}{2} \right),$$

$$\bar{\nu} = \bar{\mu} = 0$$

$$R_{\bar{\nu}, 0}^{(0)} + i \int_{\bar{\nu}, 0}^{(0)} = \frac{2}{\pi} \int_{\bar{\nu}-\frac{1}{2}}^{\bar{\nu}+\frac{1}{2}} e^{-i\bar{k}_1 X} \left[ J_0 \left( \frac{\bar{k}_1}{M} X \right) \left( \sin^{-1} \frac{2\bar{\nu}-1}{2X} - \frac{X}{2} \right) + \sum_{r=1}^{\infty} \frac{(-1)^r}{r} J_{2r} \left( \frac{\bar{k}_1}{M} X \right) \sin(2r \sin^{-1} \frac{2\bar{\nu}-1}{2X}) \right] dX,$$

$$\bar{\nu} = \bar{\mu} \geq 1$$

$$R_{\bar{\nu}, 0}^{(0)} + i \int_{\bar{\nu}, 0}^{(0)} = -\frac{4}{\pi} \int_{\bar{\nu}-\frac{1}{2}}^{\bar{\nu}+\frac{1}{2}} e^{-i\bar{k}_1 X} \left[ J_0 \left( \frac{\bar{k}_1}{M} X \right) \sin^{-1} \frac{1}{2X} + \sum_{r=1}^{\infty} \frac{(-1)^r}{r} J_{2r} \left( \frac{\bar{k}_1}{M} X \right) \sin(2r \sin^{-1} \frac{1}{2X}) \right] dX,$$

$$\bar{\nu} \geq 1, \bar{\mu} = 0$$

$$R_{\bar{\nu}, \bar{\mu}}^{(0)} + i \int_{\bar{\nu}, \bar{\mu}}^{(0)} = \frac{2}{\pi} \int_{\bar{\nu}-\frac{1}{2}}^{\bar{\nu}+\frac{1}{2}} e^{-i\bar{k}_1 X} \left[ J_0 \left( \frac{\bar{k}_1}{M} X \right) \left\{ \sin^{-1} \frac{2\bar{\mu}-1}{2X} - \sin^{-1} \frac{2\bar{\mu}+1}{2X} \right\} \right.$$

$$\left. + \sum_{r=1}^{\infty} \frac{(-1)^r}{r} J_{2r} \left( \frac{\bar{k}_1}{M} X \right) \left\{ \sin(2r \sin^{-1} \frac{2\bar{\mu}-1}{2X}) - \sin(2r \sin^{-1} \frac{2\bar{\mu}+1}{2X}) \right\} \right] dX,$$

$$\bar{\nu} > \bar{\mu} \geq 1 \text{ Eqs. (A.11a-d)}$$

# CONFIDENTIAL

where  $\bar{k}_1$  is a reduced frequency based on the streamwise dimension of a box

$$\bar{k}_1 = \frac{\omega b_1 M^2}{U \beta^2}$$

Eq. (A.12)

and  $J_{2r}$  is the Bessel function of the first kind of order  $2r$ . The function  $f_0$  is commonly encountered in linearized unsteady supersonic flow (cf. Refs. 9, 15). Although the expressions seem rather lengthy and complicated, the task of tabulating these coefficients is not difficult, because of the rapid convergence of the infinite series. (It is assumed that high-speed computers will be available.) The sine functions in the series may be written in terms of the Chebyshev polynomials  $S_n(x)$  (Ref. 10)

$$\sin(2r \sin^{-1} x) = (-1)^{r+1} \sqrt{1-x^2} S'_{2r-1}(2x)$$

Eq. (A.13)

## b. Approximate Expressions

For Mach boxes, the approximate expressions for the pressure influence coefficients are next given. These involve the same degree of approximation as those of Ref. 2 for square boxes.

$$R_{\theta,0} + iJ_{\theta,0} \approx \left\{ -1 + \frac{3}{16} \left(\frac{\bar{k}_1}{M}\right)^2 - \frac{5(4M^2+3)}{3072} \left(\frac{\bar{k}_1}{M}\right)^4 \right\} + \frac{i}{M} \left\{ \frac{1}{2} \left(\frac{\bar{k}_1}{M}\right) - \frac{(4M^2+1)}{96} \left(\frac{\bar{k}_1}{M}\right)^3 \right\}, \quad \bar{v} = \bar{\mu} = 0$$

$$R_{\bar{v},\bar{v}} + iJ_{\bar{v},\bar{v}} \approx \left\{ -\frac{\bar{k}_1 \beta^2}{\pi M^2} \sin(\bar{v}\bar{k}_1) B_{\bar{v},\bar{v}} - \frac{1}{\pi} \cos\left(\bar{v} + \frac{1}{2}\right)\bar{k}_1 \cos\left(\frac{\bar{k}_1}{M} \sqrt{\bar{v} + \frac{1}{4}}\right) A_{\bar{v},\bar{v}}^+ + \frac{1}{\pi} \cos\left(\bar{v} - \frac{1}{2}\right)\bar{k}_1 A_{\bar{v},\bar{v}}^- \right\} \\ + i \left\{ -\frac{\bar{k}_1 \beta^2}{\pi M^2} \cos(\bar{v}\bar{k}_1) B_{\bar{v},\bar{v}} + \frac{1}{\pi} \sin\left(\bar{v} + \frac{1}{2}\right)\bar{k}_1 \cos\left(\frac{\bar{k}_1}{M} \sqrt{\bar{v} + \frac{1}{4}}\right) A_{\bar{v},\bar{v}}^+ - \frac{1}{\pi} \sin\left(\bar{v} - \frac{1}{2}\right)\bar{k}_1 A_{\bar{v},\bar{v}}^- \right\},$$

$\bar{v} = \bar{\mu} \geq 2$

$$R_{\bar{v},\bar{\mu}} + iJ_{\bar{v},\bar{\mu}} \approx \left\{ \frac{\bar{k}_1 \beta^2}{\pi M^2} \sin(\bar{v}\bar{k}_1) \cos\left(\frac{\bar{k}_1}{M} \sqrt{\bar{v}^2 - \bar{\mu}^2}\right) B_{\bar{v},\bar{\mu}} - \frac{1}{\pi} \cos\left(\bar{v} + \frac{1}{2}\right)\bar{k}_1 \cos\left(\frac{\bar{k}_1}{M} \sqrt{\bar{v} + \frac{1}{4}}\right) A_{\bar{v},\bar{\mu}}^+ \right. \\ \left. + \frac{1}{\pi} \cos\left(\bar{v} - \frac{1}{2}\right)\bar{k}_1 \cos\left(\frac{\bar{k}_1}{M} \sqrt{\bar{v} - \frac{1}{4}}\right) A_{\bar{v},\bar{\mu}}^- \right\} + i \left\{ -\frac{\bar{k}_1 \beta^2}{\pi M^2} \cos(\bar{v}\bar{k}_1) \cos\left(\frac{\bar{k}_1}{M} \sqrt{\bar{v}^2 - \bar{\mu}^2}\right) B_{\bar{v},\bar{\mu}} \right. \\ \left. + \frac{1}{\pi} \sin\left(\bar{v} + \frac{1}{2}\right)\bar{k}_1 \cos\left(\frac{\bar{k}_1}{M} \sqrt{\bar{v} + \frac{1}{4}}\right) A_{\bar{v},\bar{\mu}}^+ - \frac{1}{\pi} \sin\left(\bar{v} - \frac{1}{2}\right)\bar{k}_1 \cos\left(\frac{\bar{k}_1}{M} \sqrt{\bar{v} - \frac{1}{4}}\right) A_{\bar{v},\bar{\mu}}^- \right\}$$

$\bar{v} > \bar{\mu} \geq 2$

Eqs. (A.14a-c)

# CONFIDENTIAL

where

$$\left. \begin{aligned} A_{\bar{v},0}^+ &= \pi - 2 \cos^{-1} \frac{1}{2\bar{v}+1}, \quad A_{\bar{v},0}^- = \pi - 2 \cos^{-1} \frac{1}{2\bar{v}-1} = A_{\bar{v},0}^+, \\ B_{\bar{v},0} &= \cosh^{-1}(\bar{\mu}+1) - \cosh^{-1}(2\bar{v}-1) + (\bar{v} + \frac{1}{2}) A_{\bar{v},0}^+ - (\bar{v} - \frac{1}{2}) A_{\bar{v},0}^-, \end{aligned} \right\} \bar{v} > 2, \bar{\mu} = 0$$

$$\left. \begin{aligned} A_{\bar{v},\bar{v}}^+ &= \cos^{-1} \frac{2\bar{v}-1}{2\bar{v}+1}, \quad A_{\bar{v},\bar{v}}^- = 0, \\ B_{\bar{v},\bar{v}} &= -(\bar{v} - \frac{1}{2}) \cosh^{-1} \frac{2\bar{v}+1}{2\bar{v}-1} + (\bar{v} + \frac{1}{2}) A_{\bar{v},\bar{v}}^+, \end{aligned} \right\} \bar{v} = \bar{\mu} > 2$$

$$\left. \begin{aligned} A_{\bar{v},\bar{\mu}}^+ &= \cos^{-1} \frac{2\bar{\mu}-1}{2\bar{v}+1} - \cos^{-1} \frac{2\bar{\mu}+1}{2\bar{v}+1}, \quad A_{\bar{v},\bar{\mu}}^- = \cos^{-1} \frac{2\bar{\mu}-1}{2\bar{v}-1} - \cos^{-1} \frac{2\bar{\mu}+1}{2\bar{v}-1} = A_{\bar{v},\bar{\mu}}^+, \\ B_{\bar{v},\bar{\mu}} &= (\bar{\mu} + \frac{1}{2}) \left[ \cosh^{-1} \frac{2\bar{v}+1}{2\bar{\mu}+1} - \cosh^{-1} \frac{2\bar{v}-1}{2\bar{\mu}+1} \right] - (\bar{\mu} - \frac{1}{2}) \left[ \cosh^{-1} \frac{2\bar{v}+1}{2\bar{\mu}-1} - \cosh^{-1} \frac{2\bar{v}-1}{2\bar{\mu}-1} \right] \\ &\quad + (\bar{v} + \frac{1}{2}) A_{\bar{v},\bar{\mu}}^+ - (\bar{v} - \frac{1}{2}) A_{\bar{v},\bar{\mu}}^-. \end{aligned} \right\} \begin{array}{l} \bar{v} > 2 \\ \bar{v} > \bar{\mu} > 1 \end{array}$$

(The interpretations of  $\cos^{-1}$ ,  $\cosh^{-1}$ , etc. given by Eqs. (2.10a-h), Ref. 1, have been applied.)

For the boxes in row  $\bar{v} = 1$ , a subdivision is employed which is similar to the method of Ref. 2. Referring to Fig. A.2, each such box is divided by a finer grid of  $5 \times 5$  elements.

$$R_{1,0} + iJ_{1,0} \approx \sum_{\bar{v}=3}^7 (R_{\bar{v},0} + iJ_{\bar{v},0})_{\frac{1}{5}} + 2 \sum_{\bar{v}=3}^7 \sum_{\bar{\mu}=1}^2 (R_{\bar{v},\bar{\mu}} + iJ_{\bar{v},\bar{\mu}})_{\frac{1}{5}}, \quad \bar{v} = 1, \bar{\mu} = 0$$

$$R_{1,1} + iJ_{1,1} \approx \sum_{\bar{v}=3}^7 \sum_{\bar{\mu}=3}^7 (R_{\bar{v},\bar{\mu}} + iJ_{\bar{v},\bar{\mu}})_{\frac{1}{5}}, \quad \bar{v} = \bar{\mu} = 1$$

Eqs. (A.14d-e)

where the subscript indicates that  $R_{\bar{v},\bar{\mu}} + iJ_{\bar{v},\bar{\mu}}$  depend on a reduced frequency argument equal to one fifth of  $\bar{v}$ , and are obtainable from Eqs. (A.14a-c).

As may be seen from the definitions,  $A_{\bar{v},\bar{\mu}}^+$ ,  $A_{\bar{v},\bar{\mu}}^-$  and  $B_{\bar{v},\bar{\mu}}$  are independent of Mach number, in contrast to the

# CONFIDENTIAL

corresponding coefficients for the square box scheme. The Mach box tabulations are therefore much simpler. The values of

$A_{\bar{v}, \bar{\mu}}^+$ ,  $A_{\bar{v}, \bar{\mu}}^-$  and  $B_{\bar{v}, \bar{\mu}}$  are given in Table A.1 for  $\bar{v}$  from 2 to 25 and for  $\bar{\mu}$  from 0 to 25. Note that only values of  $\bar{\mu} \leq \bar{v}$  need be considered. For the steady case, the above formulas are exact. A short table of  $R_{\bar{v}, \bar{\mu}} (k=0)$  is also included (Table A.2).

For the velocity-potential-difference influence coefficients, the following approximate formulas apply:

$$R_{0,0}^{(\varphi)} + i J_{0,0}^{(\varphi)} \approx \left\{ -1 + \frac{2M^2+1}{48} \left(\frac{\bar{k}_1}{M}\right)^2 - \frac{8M^4+24M^2+3}{15,360} \left(\frac{\bar{k}_1}{M}\right)^4 \right\} + iM \left\{ \frac{1}{4} \left(\frac{\bar{k}_1}{M}\right) - \frac{2M^2+3}{384} \left(\frac{\bar{k}_1}{M}\right)^3 \right\}, \quad \bar{v} = \bar{\mu} = 0$$

$$R_{\bar{v}, \bar{\mu}}^{(\varphi)} + i J_{\bar{v}, \bar{\mu}}^{(\varphi)} \approx -\frac{2}{\pi} (\cos \bar{v} \bar{k}_1 - i \sin \bar{v} \bar{k}_1) \cos \left( \frac{\bar{k}_1}{M} \sqrt{\bar{v}^2 - \bar{\mu}^2} \right) B_{\bar{v}, \bar{\mu}}, \quad \bar{v} \geq \bar{\mu} \geq 2$$

$$R_{1,0}^{(\varphi)} + i J_{1,0}^{(\varphi)} \approx \frac{1}{5} \sum_{\bar{v}=1}^7 (R_{\bar{v},0}^{(\varphi)} + i J_{\bar{v},0}^{(\varphi)}) \frac{\bar{k}_1}{5} + \frac{2}{5} \sum_{\bar{v}=3}^7 \sum_{\bar{\mu}=1}^2 (R_{\bar{v},\bar{\mu}}^{(\varphi)} + i J_{\bar{v},\bar{\mu}}^{(\varphi)}) \frac{\bar{k}_1}{5}, \quad \bar{v}=1, \bar{\mu}=0$$

$$R_{1,1}^{(\varphi)} + i J_{1,1}^{(\varphi)} \approx \frac{1}{5} \sum_{\bar{v}=3}^7 \sum_{\bar{\mu}=3}^{\bar{v}} (R_{\bar{v},\bar{\mu}}^{(\varphi)} + i J_{\bar{v},\bar{\mu}}^{(\varphi)}) \frac{\bar{k}_1}{5}, \quad \bar{v} = \bar{\mu} = 1$$

Eqs. (A.15a-d)

CONFIDENTIAL

TABLE A.1 TABULATION OF  $J_{1/2}$

$x$	0	1	2	3	4	5	6	7	8	9	10	11	12	13
2	0.432,715,5	0.442,145,2	0.527,855,2	0.775,181,3										
3	0.266,565,1	0.269,561,3	0.252,561,3	0.192,081,9										
4	0.222,582,0	0.228,495,9	0.249,194,1	0.342,081,9										
5	0.182,059,6	0.195,192,0	0.195,425,2	0.217,513,1	0.679,871,7									
6	0.153,996,3	0.155,824,1	0.154,922,9	0.173,519,2	0.244,044,5	0.612,554,7								
7	0.131,412,3	0.134,641,8	0.138,479,6	0.145,638,3	0.152,682,9	0.179,710,9	0.522,314,8							
8	0.117,715,0	0.116,542,2	0.121,132,6	0.125,177,5	0.133,517,3	0.145,813,5	0.162,072,5	0.429,975,3						
9	0.105,311,8	0.105,902,3	0.107,335,9	0.111,085,6	0.116,159,3	0.123,967,7	0.136,061,3	0.152,254,2	0.176,556,5					
10	0.094,744,1	0.097,756,5	0.097,956,5	0.099,432,7	0.102,194,8	0.106,495,9	0.116,112,5	0.125,873,5	0.137,879,8	0.149,379,9				
11	0.084,903,9	0.087,316,5	0.086,533,6	0.089,112,6	0.092,194,8	0.094,524,9	0.098,023,3	0.101,711,9	0.104,329,8	0.106,891,5	0.109,370,2			
12	0.076,081,3	0.078,275,6	0.077,493,2	0.079,391,9	0.081,434,2	0.082,436,2	0.083,388,3	0.084,299,8	0.085,171,9	0.085,991,5	0.086,766,5	0.102,112,4		
13	0.068,979,2	0.069,144,2	0.069,645,9	0.070,507,4	0.071,762,8	0.073,495,0	0.075,784,5	0.078,638,9	0.081,958,4	0.085,742,8	0.089,920,6	0.104,309,2	0.120,737,2	
14	0.061,527,3	0.059,662,2	0.055,072,1	0.045,772,9	0.036,732,1	0.028,177,7	0.020,992,9	0.014,921,5	0.010,241,9	0.007,285,4	0.005,029,8	0.003,519,1	0.002,715,8	0.002,157,896,3
15	0.056,015,3	0.050,727,1	0.041,652,9	0.031,684,2	0.022,481,5	0.015,513,2	0.010,076,7	0.006,549,3	0.004,494,3	0.003,222,5	0.002,246,0	0.001,585,6	0.001,173,8	0.000,859,3
16	0.051,150,6	0.043,244,3	0.033,258,0	0.023,082,2	0.015,786,5	0.010,559,5	0.006,863,0	0.004,564,0	0.003,069,0	0.002,066,3	0.001,385,7	0.000,919,0	0.000,628,2	0.000,450,4
17	0.047,130,6	0.037,244,3	0.027,158,0	0.018,082,2	0.011,786,5	0.007,559,5	0.004,863,0	0.003,064,0	0.001,969,0	0.001,288,7	0.000,819,0	0.000,528,2	0.000,357,7	0.000,259,4
18	0.043,950,6	0.033,126,3	0.023,040,0	0.014,964,2	0.009,786,5	0.006,559,5	0.004,264,0	0.002,569,0	0.001,674,0	0.001,093,8	0.000,624,0	0.000,357,7	0.000,228,2	0.000,159,6
19	0.041,288,2	0.031,126,3	0.021,050,0	0.013,974,2	0.009,796,2	0.006,563,4	0.004,269,0	0.002,574,0	0.001,679,0	0.001,098,9	0.000,629,0	0.000,360,0	0.000,231,0	0.000,162,0
20	0.038,785,3	0.028,623,5	0.018,547,2	0.011,471,4	0.007,285,2	0.004,990,2	0.003,295,0	0.002,000,0	0.001,305,0	0.000,820,0	0.000,525,0	0.000,330,0	0.000,215,0	0.000,146,0
21	0.036,515,3	0.026,353,5	0.016,277,2	0.009,201,4	0.005,015,2	0.003,320,0	0.002,025,0	0.001,330,0	0.000,845,0	0.000,550,0	0.000,355,0	0.000,240,0	0.000,155,0	0.000,100,0
22	0.034,448,1	0.024,286,3	0.014,210,0	0.007,134,2	0.003,049,0	0.001,954,0	0.001,259,0	0.000,774,0	0.000,479,0	0.000,284,0	0.000,169,0	0.000,104,0	0.000,079,0	0.000,054,0
23	0.032,556,4	0.022,394,6	0.012,318,3	0.005,252,2	0.002,163,0	0.001,468,0	0.000,983,0	0.000,688,0	0.000,493,0	0.000,308,0	0.000,193,0	0.000,128,0	0.000,093,0	0.000,068,0
24	0.030,819,2	0.020,657,4	0.010,581,1	0.003,376,0	0.001,490,0	0.001,005,0	0.000,710,0	0.000,515,0	0.000,330,0	0.000,215,0	0.000,150,0	0.000,105,0	0.000,080,0	0.000,055,0
25	0.029,218,2	0.019,056,4	0.009,980,1	0.002,498,0	0.001,112,0	0.000,817,0	0.000,622,0	0.000,427,0	0.000,242,0	0.000,157,0	0.000,102,0	0.000,077,0	0.000,052,0	0.000,037,0

CONFIDENTIAL

CONFIDENTIAL

TABLE A.1 (CONTINUED) TABULATION OF  $A_{12}$

	14	15	16	17	18	19	20	21	22	23	24	25
2	0.579,673.8	1,233,959.4	0									
3	0.402,715.8	0.442,183.2	0.927,205.2	0								
4	0.286,695.1	0.259,563.5	0.522,591.9	0.775,193.3	0							
5	0.222,122.0	0.228,195.9	0.289,194.1	0.302,091.6	0.578,673.7	0						
6	0.182,069.6	0.185,192.0	0.195,635.2	0.217,913.1	0.268,166.6	0.512,554.7	0					
7	0.153,958.3	0.155,969.1	0.151,922.9	0.173,819.2	0.196,071.8	0.244,044.5	0.562,065.3	0				
8	0.133,432.3	0.134,641.8	0.138,475.9	0.157,952.9	0.175,710.9	0.195,269.5	0.225,269.5	0.252,311.3	0			
9	0.117,715.0	0.118,542.2	0.121,132.6	0.128,597.5	0.133,952.9	0.145,813.5	0.156,864.7	0.166,864.7	0.179,577.3	0		
10	0.105,311.8	0.105,922.3	0.107,735.9	0.111,045.0	0.112,212.5	0.115,159.2	0.118,073.5	0.120,830.5	0.123,590.5	0.127,350.5	0	
11	0.095,274.1	0.095,470.6	0.097,470.6	0.099,436.7	0.102,374.2	0.105,284.9	0.108,182.3	0.110,062.3	0.111,928.3	0.113,789.3	0	
12	0.085,983.3	0.087,315.5	0.088,333.6	0.091,112.0	0.092,774.2	0.094,475.8	0.096,223.3	0.098,023.3	0.099,800.6	0.101,559.5	0	
13	0.078,091.0	0.078,295.6	0.079,019.3	0.080,279.2	0.081,584.2	0.082,934.2	0.084,334.2	0.085,784.2	0.087,284.2	0.088,834.2	0	
14	0.074,379.2	0.074,420.5	0.074,414.2	0.074,358.2	0.074,258.0	0.074,112.0	0.073,928.0	0.073,808.0	0.073,748.0	0.073,748.0	0.073,748.0	0
15	0.064,527.3	0.064,662.2	0.065,072.1	0.065,772.9	0.066,773.1	0.067,773.1	0.068,773.1	0.069,773.1	0.070,773.1	0.071,773.1	0.072,773.1	0
16	0.060,515.3	0.060,727.1	0.061,052.2	0.061,584.2	0.062,324.2	0.063,264.2	0.064,304.2	0.065,444.2	0.066,684.2	0.068,024.2	0.069,464.2	0
17	0.057,150.6	0.057,244.3	0.057,328.0	0.057,402.0	0.057,466.0	0.057,520.0	0.057,564.0	0.057,608.0	0.057,652.0	0.057,696.0	0.057,740.0	0
18	0.054,060.6	0.054,139.9	0.054,209.9	0.054,279.9	0.054,349.9	0.054,419.9	0.054,489.9	0.054,559.9	0.054,629.9	0.054,699.9	0.054,769.9	0
19	0.051,238.2	0.051,325.3	0.051,409.3	0.051,493.3	0.051,577.3	0.051,661.3	0.051,745.3	0.051,829.3	0.051,913.3	0.051,997.3	0.052,081.3	0
20	0.048,785.2	0.048,846.2	0.048,907.2	0.048,968.2	0.049,029.2	0.049,090.2	0.049,151.2	0.049,212.2	0.049,273.2	0.049,334.2	0.049,395.2	0
21	0.046,515.3	0.046,566.2	0.046,617.2	0.046,668.2	0.046,719.2	0.046,770.2	0.046,821.2	0.046,872.2	0.046,923.2	0.046,974.2	0.047,025.2	0
22	0.044,442.1	0.044,492.1	0.044,542.1	0.044,592.1	0.044,642.1	0.044,692.1	0.044,742.1	0.044,792.1	0.044,842.1	0.044,892.1	0.044,942.1	0
23	0.042,556.4	0.042,595.3	0.042,634.2	0.042,673.1	0.042,712.0	0.042,750.9	0.042,789.8	0.042,828.7	0.042,867.6	0.042,906.5	0.042,945.4	0
24	0.040,819.2	0.040,853.1	0.040,887.0	0.040,920.9	0.040,954.8	0.040,988.7	0.041,022.6	0.041,056.5	0.041,090.4	0.041,124.3	0.041,158.2	0
25	0.373,555.9	0.351,170.4	0.349,536.0	0								
14	0.152,857.4	0	0	0	0.330,287.3	0						
15	0.115,074.6	0.117,542.1	0.113,073.4	0.138,267.6	0.155,233.0	0.132,641.0	0.113,631.2	0				
16	0.095,452.2	0.111,479.1	0.108,200.9	0.138,267.6	0.155,233.0	0.132,641.0	0.113,631.2	0				
17	0.082,868.8	0.094,575.1	0.108,200.9	0.138,267.6	0.155,233.0	0.132,641.0	0.113,631.2	0				
18	0.073,741.1	0.080,373.1	0.095,395.6	0.125,395.6	0.155,233.0	0.132,641.0	0.113,631.2	0				
19	0.066,823.1	0.071,634.0	0.078,140.4	0.095,395.6	0.125,395.6	0.155,233.0	0.132,641.0	0				
20	0.061,316.0	0.064,966.9	0.069,697.7	0.076,084.1	0.085,256.3	0.094,367.8	0.103,426.3	0.109,467.8	0.115,566.7	0.121,625.2	0.127,645.7	0
21	0.056,735.4	0.059,628.6	0.063,526.9	0.067,910.6	0.074,131.9	0.081,177.1	0.087,950.4	0.094,492.9	0.100,842.9	0.107,042.9	0.113,142.9	0
22	0.052,997.8	0.055,300.5	0.058,128.7	0.061,675.4	0.066,254.0	0.072,115.7	0.078,115.7	0.084,321.5	0.090,721.5	0.097,321.5	0.104,121.5	0
23	0.049,749.0	0.051,528.6	0.053,917.9	0.056,710.9	0.060,226.5	0.065,713.3	0.071,395.9	0.077,321.5	0.083,521.5	0.089,921.5	0.096,521.5	0
24	0.046,829.2	0.048,528.1	0.050,326.0	0.052,125.9	0.054,125.9	0.056,325.9	0.058,725.9	0.061,325.9	0.064,125.9	0.067,125.9	0.070,325.9	0
25	0.044,159.2	0.045,858.1	0.047,656.0	0.049,455.9	0.051,455.9	0.053,655.9	0.056,055.9	0.058,655.9	0.061,455.9	0.064,455.9	0.067,655.9	0

	14	15	16	17	18	19	20	21	22	23	24	25
14	0											
15	0.373,555.9	0.351,170.4	0.349,536.0	0								
16	0.152,857.4	0	0	0	0.330,287.3	0						
17	0.115,074.6	0.117,542.1	0.113,073.4	0.138,267.6	0.155,233.0	0.132,641.0	0.113,631.2	0				
18	0.095,452.2	0.111,479.1	0.108,200.9	0.138,267.6	0.155,233.0	0.132,641.0	0.113,631.2	0				
19	0.082,868.8	0.094,575.1	0.108,200.9	0.138,267.6	0.155,233.0	0.132,641.0	0.113,631.2	0				
20	0.073,741.1	0.080,373.1	0.095,395.6	0.125,395.6	0.155,233.0	0.132,641.0	0.113,631.2	0				
21	0.066,823.1	0.071,634.0	0.078,140.4	0.095,395.6	0.125,395.6	0.155,233.0	0.132,641.0	0				
22	0.061,316.0	0.064,966.9	0.069,697.7	0.076,084.1	0.085,256.3	0.094,367.8	0.103,426.3	0.109,467.8	0.115,566.7	0.121,625.2	0.127,645.7	0
23	0.056,735.4	0.059,628.6	0.063,526.9	0.067,910.6	0.074,131.9	0.081,177.1	0.087,950.4	0.094,492.9	0.100,842.9	0.107,042.9	0.113,142.9	0
24	0.052,997.8	0.055,300.5	0.058,128.7	0.061,675.4	0.066,254.0	0.072,115.7	0.078,115.7	0.084,321.5	0.090,721.5	0.097,321.5	0.104,121.5	0
25	0.049,749.0	0.051,528.6	0.053,917.9	0.056,710.9	0.060,226.5	0.065,713.3	0.071,395.9	0.077,321.5	0.083,521.5	0.089,921.5	0.096,521.5	0

CONFIDENTIAL

TABLE A.1 (CONTINUED) TABULATION OF  $S_{12}$

	0	1	2	3	4	5	6	7	8	9	10	11	12	13
2	0.516,963.4	0.611,999.9	0.670,339.7	0.705,639.8	0.722,079.1	0.732,000.3	0.736,125.0	0.736,302.8	0.733,444.9	0.728,442.4	0.721,068.3	0.712,287.2	0.702,932.9	0.693,529.0
3	0.338,127.5	0.360,948.2	0.405,144.5	0.417,985.7	0.472,079.1	0.422,000.3	0.365,125.0	0.285,872.9	0.253,442.4	0.214,371.9	0.153,325.6	0.136,738.4	0.111,029.7	0.085,529.3
4	0.251,991.3	0.260,708.1	0.289,065.1	0.289,065.1	0.368,455.7	0.422,000.3	0.365,125.0	0.285,872.9	0.253,442.4	0.214,371.9	0.153,325.6	0.136,738.4	0.111,029.7	0.085,529.3
5	0.201,012.4	0.205,875.0	0.228,065.9	0.228,065.9	0.368,455.7	0.422,000.3	0.365,125.0	0.285,872.9	0.253,442.4	0.214,371.9	0.153,325.6	0.136,738.4	0.111,029.7	0.085,529.3
6	0.167,230.3	0.159,675.0	0.177,623.7	0.177,623.7	0.368,455.7	0.422,000.3	0.365,125.0	0.285,872.9	0.253,442.4	0.214,371.9	0.153,325.6	0.136,738.4	0.111,029.7	0.085,529.3
7	0.143,223.8	0.144,731.7	0.149,568.1	0.149,568.1	0.368,455.7	0.422,000.3	0.365,125.0	0.285,872.9	0.253,442.4	0.214,371.9	0.153,325.6	0.136,738.4	0.111,029.7	0.085,529.3
8	0.125,205.3	0.126,240.4	0.129,405.8	0.129,405.8	0.368,455.7	0.422,000.3	0.365,125.0	0.285,872.9	0.253,442.4	0.214,371.9	0.153,325.6	0.136,738.4	0.111,029.7	0.085,529.3
9	0.111,283.3	0.111,283.3	0.110,635.5	0.110,635.5	0.368,455.7	0.422,000.3	0.365,125.0	0.285,872.9	0.253,442.4	0.214,371.9	0.153,325.6	0.136,738.4	0.111,029.7	0.085,529.3
10	0.100,125.3	0.100,125.3	0.100,125.3	0.100,125.3	0.368,455.7	0.422,000.3	0.365,125.0	0.285,872.9	0.253,442.4	0.214,371.9	0.153,325.6	0.136,738.4	0.111,029.7	0.085,529.3
11	0.091,003.3	0.091,003.3	0.091,003.3	0.091,003.3	0.368,455.7	0.422,000.3	0.365,125.0	0.285,872.9	0.253,442.4	0.214,371.9	0.153,325.6	0.136,738.4	0.111,029.7	0.085,529.3
12	0.083,405.8	0.083,405.8	0.083,405.8	0.083,405.8	0.368,455.7	0.422,000.3	0.365,125.0	0.285,872.9	0.253,442.4	0.214,371.9	0.153,325.6	0.136,738.4	0.111,029.7	0.085,529.3
13	0.076,940.1	0.076,940.1	0.076,940.1	0.076,940.1	0.368,455.7	0.422,000.3	0.365,125.0	0.285,872.9	0.253,442.4	0.214,371.9	0.153,325.6	0.136,738.4	0.111,029.7	0.085,529.3
14	0.071,474.2	0.071,474.2	0.071,474.2	0.071,474.2	0.368,455.7	0.422,000.3	0.365,125.0	0.285,872.9	0.253,442.4	0.214,371.9	0.153,325.6	0.136,738.4	0.111,029.7	0.085,529.3
15	0.066,703.9	0.066,703.9	0.066,703.9	0.066,703.9	0.368,455.7	0.422,000.3	0.365,125.0	0.285,872.9	0.253,442.4	0.214,371.9	0.153,325.6	0.136,738.4	0.111,029.7	0.085,529.3
16	0.062,530.4	0.062,530.4	0.062,530.4	0.062,530.4	0.368,455.7	0.422,000.3	0.365,125.0	0.285,872.9	0.253,442.4	0.214,371.9	0.153,325.6	0.136,738.4	0.111,029.7	0.085,529.3
17	0.058,849.0	0.058,849.0	0.058,849.0	0.058,849.0	0.368,455.7	0.422,000.3	0.365,125.0	0.285,872.9	0.253,442.4	0.214,371.9	0.153,325.6	0.136,738.4	0.111,029.7	0.085,529.3
18	0.055,577.0	0.055,577.0	0.055,577.0	0.055,577.0	0.368,455.7	0.422,000.3	0.365,125.0	0.285,872.9	0.253,442.4	0.214,371.9	0.153,325.6	0.136,738.4	0.111,029.7	0.085,529.3
19	0.052,659.8	0.052,659.8	0.052,659.8	0.052,659.8	0.368,455.7	0.422,000.3	0.365,125.0	0.285,872.9	0.253,442.4	0.214,371.9	0.153,325.6	0.136,738.4	0.111,029.7	0.085,529.3
20	0.050,005.6	0.050,005.6	0.050,005.6	0.050,005.6	0.368,455.7	0.422,000.3	0.365,125.0	0.285,872.9	0.253,442.4	0.214,371.9	0.153,325.6	0.136,738.4	0.111,029.7	0.085,529.3
21	0.047,632.6	0.047,632.6	0.047,632.6	0.047,632.6	0.368,455.7	0.422,000.3	0.365,125.0	0.285,872.9	0.253,442.4	0.214,371.9	0.153,325.6	0.136,738.4	0.111,029.7	0.085,529.3
22	0.045,466.2	0.045,466.2	0.045,466.2	0.045,466.2	0.368,455.7	0.422,000.3	0.365,125.0	0.285,872.9	0.253,442.4	0.214,371.9	0.153,325.6	0.136,738.4	0.111,029.7	0.085,529.3
23	0.043,408.6	0.043,408.6	0.043,408.6	0.043,408.6	0.368,455.7	0.422,000.3	0.365,125.0	0.285,872.9	0.253,442.4	0.214,371.9	0.153,325.6	0.136,738.4	0.111,029.7	0.085,529.3
24	0.041,457.7	0.041,457.7	0.041,457.7	0.041,457.7	0.368,455.7	0.422,000.3	0.365,125.0	0.285,872.9	0.253,442.4	0.214,371.9	0.153,325.6	0.136,738.4	0.111,029.7	0.085,529.3
25	0.040,008.0	0.040,008.0	0.040,008.0	0.040,008.0	0.368,455.7	0.422,000.3	0.365,125.0	0.285,872.9	0.253,442.4	0.214,371.9	0.153,325.6	0.136,738.4	0.111,029.7	0.085,529.3

	14	15	16	17	18	19	20	21	22	23	24	25	
14	0.252,001.6	0.253,457.1	0.255,122.8	0.256,981.2	0.258,935.1	0.260,981.2	0.263,119.1	0.265,349.7	0.267,671.9	0.270,085.7	0.272,591.2	0.275,188.4	0.277,877.1
15	0.205,170.4	0.195,290.2	0.185,444.8	0.175,629.8	0.165,841.8	0.156,078.2	0.146,438.2	0.136,912.2	0.127,490.2	0.118,172.2	0.108,958.2	0.099,848.2	0.090,842.2
16	0.131,291.0	0.127,174.8	0.122,987.2	0.118,821.8	0.114,686.5	0.110,571.3	0.106,476.2	0.102,391.2	0.098,316.2	0.094,251.2	0.090,196.2	0.086,151.2	0.082,116.2
17	0.104,445.4	0.101,427.6	0.098,325.5	0.095,230.7	0.092,145.8	0.089,060.9	0.085,976.0	0.082,891.1	0.079,806.2	0.076,721.3	0.073,636.4	0.070,551.5	0.067,466.6
18	0.088,745.6	0.086,475.1	0.084,204.6	0.081,934.1	0.079,663.6	0.077,393.1	0.075,122.6	0.072,852.1	0.070,581.6	0.068,311.1	0.066,040.6	0.063,770.1	0.061,500.6
19	0.078,052.0	0.076,781.5	0.075,511.0	0.074,240.5	0.072,970.0	0.071,700.5	0.070,430.0	0.069,160.5	0.067,890.0	0.066,620.5	0.065,350.0	0.064,080.5	0.062,810.0
20	0.070,138.0	0.069,785.0	0.069,432.0	0.069,079.0	0.068,726.0	0.068,373.0	0.068,020.0	0.067,667.0	0.067,314.0	0.066,961.0	0.066,608.0	0.066,255.0	0.065,902.0
21	0.065,970.0	0.065,720.0	0.065,470.0	0.065,220.0	0.064,970.0	0.064,720.0	0.064,470.0	0.064,220.0	0.063,970.0	0.063,720.0	0.063,470.0	0.063,220.0	0.062,970.0
22	0.062,982.0	0.062,811.0	0.062,640.0	0.062,469.0	0.062,298.0	0.062,127.0	0.061,956.0	0.061,785.0	0.061,614.0	0.061,443.0	0.061,272.0	0.061,101.0	0.060,930.0
23	0.059,186.0	0.059,114.0	0.059,042.0	0.058,970.0	0.058,898.0	0.058,826.0	0.058,754.0	0.058,682.0	0.058,610.0	0.058,538.0	0.058,466.0	0.058,394.0	0.058,322.0
24	0.057,359.0	0.057,286.0	0.057,214.0	0.057,142.0	0.057,070.0	0.057,000.0	0.056,930.0	0.056,860.0	0.056,790.0	0.056,720.0	0.056,650.0	0.056,580.0	0.056,510.0
25	0.054,831.0	0.054,758.0	0.054,686.0	0.054,614.0	0.054,542.0	0.054,470.0	0.054,400.0	0.054,330.0	0.054,260.0	0.054,190.0	0.054,120.0	0.054,050.0	0.053,980.0

TABLE A.2 TABULATION OF  $\mathcal{R}_{\nu, \mu}$  FOR STEADY-STATE CASE

$\nu$	0	1	2	3	4	5	6
0	-1.000,000,0						
1	0.783,653,1	-0.391,826,6					
2	0.088,158,5	0.251,088,0	-0.295,167,2				
3	0.036,930,5	0.045,384,5	0.182,901,9	-0.246,751,7			
4	0.020,376,0	0.022,621,5	0.032,944,4	0.150,592,9	-0.216,346,9		
5	0.012,927,3	0.013,784,1	0.017,048,3	0.026,794,9	0.130,891,3	-0.194,982,2	
6	0.008,935,4	0.009,333,8	0.010,731,0	0.014,035,5	0.023,044,0	0.117,300,5	-0.178,912,4
7	0.006,546,4	0.006,756,9	0.007,462,4	0.008,956,6	0.012,124,1	0.020,478,0	0.107,206,8
8	0.005,003,0	0.005,124,7	0.005,521,5	0.006,310,1	0.007,787,6	0.010,789,9	0.018,590,9
9	0.003,948,1	0.004,023,4	0.004,264,3	0.004,724,2	0.005,525,2	0.006,953,7	0.009,797,9
10	0.003,195,1	0.003,244,1	0.003,399,3	0.003,687,1	0.004,165,1	0.004,953,5	0.006,325,1
11	0.002,638,9	0.002,672,2	0.002,776,6	0.002,966,7	0.003,272,0	0.003,750,0	0.004,516,6
12	0.002,216,3	0.002,239,7	0.002,312,7	0.002,443,5	0.002,648,7	0.002,958,4	0.003,428,5

$\mu$	7	8	9	10	11	12
7	-0.166,258,0					
8	0.099,332,0	-0.155,958,2				
9	0.017,132,6	0.092,967,7	-0.147,363,1			
10	0.009,026,3	0.015,964,2	0.087,686,4	-0.140,048,7		
11	0.005,832,0	0.008,405,9	0.015,001,9	0.083,212,3	-0.133,725,6	
12	0.004,170,4	0.005,433,0	0.007,893,9	0.014,192,3	0.079,359,2	-0.128,188,4

# CONFIDENTIAL

## APPENDIX B

### DETERMINATION OF DOWNWASH DISTRIBUTION

In the determination of the generalized forces for use in the assumed-mode approach of flutter analysis, one must first obtain either the pressure or the velocity potential distribution over the wing due to the downwash which is associated with each of the assumed free vibration modes. The downwash  $w(x, y, t)$  corresponding to an assumed mode  $Af(x, y)$  in simple harmonic motion (complex representation) may be expressed by

$$w(x, y, t) = \frac{AU}{b} \left\{ a f(x, y) + b \frac{\partial f(x, y)}{\partial x} \right\} e^{i\omega t}$$

Eq. (B.1)

The downwash is a function of both the deflection and its streamwise slope. If the functionality of each such mode with respect to the streamwise coordinate  $x$  is known analytically, then no difficulty arises in determining the downwash at any desired point. For example, in the case of a beam-rod type structure, where there are no chordwise elastic deformations,  $f(x, y)$  is at most linear in the variable  $x$ . However, for a plate type structure, there exist chordwise elastic deformations, and one must resort to graphical differentiation or construct an analytical approximation for  $f(x, y)$  in the  $x$ -direction at a given spanwise station in order to obtain streamwise slopes.

In practice, the flutter mode is assumed to be some linear complex combination of the first few free vibration modes. For a plate structure, the frequencies and deflections at a set of discrete points are usually obtainable for these modes. The main task in evaluating the downwashes is to find the streamwise slopes and deflections at the centers of the boxes from the deflections at these given points. If, at each spanwise station corresponding to the centers of each column of boxes, there exists a sufficient number of points at which deflections can be computed, then simple graphical procedures can be resorted to to obtain the downwashes at the centers of the boxes. Otherwise, the usual procedure is to find suitable polynomial expressions for the deflections. Then the slopes are obtainable by proper differentiations of these polynomials.

#### B.1 General Procedure for Finding Approximate Analytical Expressions for the Deflections

Consider a cantilever rectangular wing on which the deflections  $f(x_i, y_j)$  are given at  $m \times n$  points as shown in Fig. B.1.

# CONFIDENTIAL

Given the deflections at  $y=y_1, \dots, y_i, \dots, y_n$  at any chordwise location  $x_i$  one can find a polynomial in  $y$  for the deflection  $f(x_i, y)$ . For this cantilever case, if the polynomial is given by

$$g(x_i, y) = b_{i2}y^2 + b_{i3}y^3 + \dots + b_{i,n+1}y^{n+1} = g_i(y), \quad \text{Eq. (B.2)}$$

then one has

$$g(x_i, y_1) = b_{i2}y_1^2 + b_{i3}y_1^3 + \dots + b_{i,n+1}y_1^{n+1}$$

$$g(x_i, y_n) = b_{i2}y_n^2 + b_{i3}y_n^3 + \dots + b_{i,n+1}y_n^{n+1}$$

Eqs. (B.3)

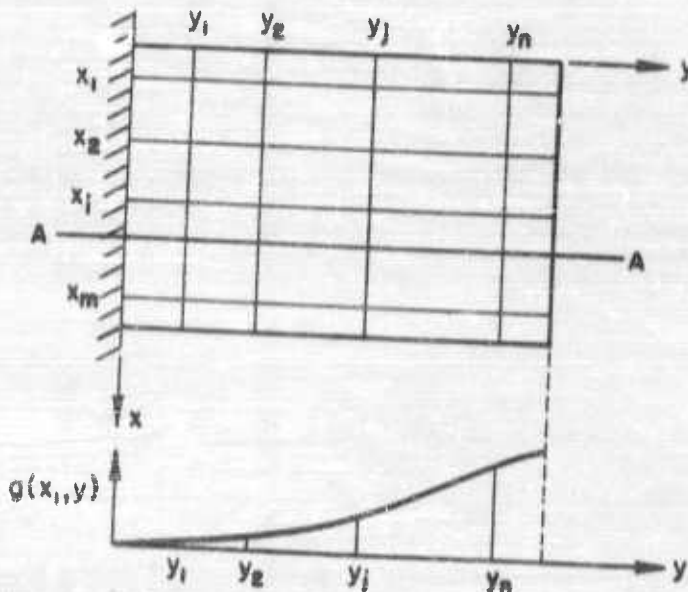


Fig. B.1 Typical Spanwise Deflection Curve

Solutions of the above set of simultaneous equations yield the constants  $b_{i2}, b_{i3}, \dots, b_{i,n+1}$ . Analytic expressions for other chordwise locations may be obtained in a similar manner. In general, the deflection over the whole surface may then be written as:

# CONFIDENTIAL

$$f(x,y) = h_1(x)g_1(y) + h_2(x)g_2(y) + \dots + h_m(x)g_m(y)$$

Eq. (B.4)

where the functions  $h_i(x)$  are polynomials in  $x$  which satisfy the relations

$$h_i(x_i) = 1, \quad h_i(x_k) = 0 \text{ when } k \neq i$$

Eqs. (B.5)

Again one may find polynomial expressions for  $h_i(x)$ . The degree of  $h_i(x)$  will depend on the number of chordwise points. Once the general form of the deflection [Eq. (B.4)] is obtained, one can easily determine the downwash at any desired point according to Eq. (B.1). It should be noted that either a graphical method or a procedure similar to the above for finding the downwash is necessary regardless of the type of grid system used.

It is worth mentioning at this point that when one finds a polynomial which passes through a given set of points  $x_1, \dots, x_m$  (or  $y_1, \dots, y_n$ ), one can be sure of its reliability only in the range  $x_1 \leq x \leq x_m$  (or  $y_1 \leq y \leq y_n$ ). Beyond these limits the polynomial may deviate considerably from the true picture. It is therefore desirable to have the  $x_1$ - and  $x_m$ -stations near the leading and trailing edges respectively, so that the chordwise locations of the boxes will not be much beyond these limits. Similarly, the centers of the boxes nearest the tip should not be much beyond  $y_n$ . To insure this in instances where the deflections at points near the edges are not given from normal mode data, some artificial means must be devised. One such means is the cross-plotting of the deflection along constant  $x$ - and constant  $y$ -lines, so that a reasonably smooth deflection surface results.

## B.2 The Triangular Wing

In essence, one might consider the above as a useful scheme for finding deflection polynomials for other planforms, such as a triangular wing. As an example, consider the oversimplified case of Fig. B.2; deflections are given at only six points. On actual wings, there will be given more points (cf. Fig. D.1), but still they will be limited to the extent that at outboard spanwise stations only one or two chordwise points will be available. For such stations, it is a difficult task to obtain accurate streamwise slopes. In order to find polynomials that fit the surface deflections of the planform, it is necessary to have artificial, reasonable estimates of the deflections at points  $a, b, c$  which may or may not lie on the planform. However, such calculations demand cut and trial cross-plotting procedures of deflection vs.  $x$  for constant values of  $y$  and of deflection vs.  $y$  for constant values of  $x$  with arbitrary extensions of curves whenever the data are lacking. The following procedure (which can be also applied to the rectangular wing as well) is suggested:

**CONFIDENTIAL**

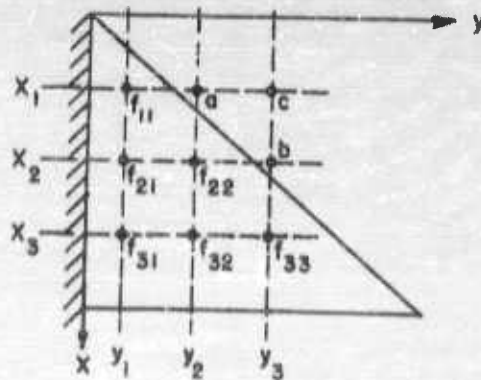


Fig. B.2 Illustrative Example for Finding the Analytical Expression of the Deflection on a Cantilever Delta Wing

(1) From the aforementioned cross-plots, find at the given sets of  $x$ 's, the deflections at the spanwise stations corresponding to the centers of various columns of boxes. When changing Mach number, the spanwise location of the boxes will not change if the span-dimension of a box is kept fixed (as suggested in Section III).

(2) Knowing the deflections at a discrete set of points for each desired spanwise station, one can proceed analytically to find polynomials in  $x$  for each such spanwise station.

(3) Using these polynomials one can differentiate to find streamwise slopes.

In the above steps, one may employ any existing additional requirements on the polynomial which would supplement the data of deflections. For instance, one can utilize the boundary conditions for the cantilever wing

$$z = 0, \quad \frac{\partial z}{\partial y} = 0 \quad \text{for all } x\text{'s at } y = 0. \quad \text{Eqs. (B.8-9)}$$

Another condition is that the trailing edge is free, so that

$$\left( \frac{\partial^2 z}{\partial x^2} + \nu \frac{\partial^2 z}{\partial y^2} \right) z = 0 \quad \text{at trailing edge. Eq. (B.10)}$$

As it stands condition (B.10) is difficult to use, so that one may take this condition approximately by setting

$$\frac{\partial^2 z}{\partial x^2} = 0 \quad \text{at trailing edge. Eq. (B.11)}$$

This is justified, since for built-up beams the effective Poisson's ratio  $\nu$  is small.

**CONFIDENTIAL**

# CONFIDENTIAL

## B.3 Lagrangian Interpolation Technique

In cases where, for each mode, both the deflections and their slopes are given for a set of discrete points, it is possible to find the deflection and its slope at any other point by direct interpolation. Then the determination of an analytic expression for the deflection is no longer required.

Given a function  $f$  at  $(2N+1)$  equally spaced points, it is possible to pass through these points a polynomial of order  $2N$

$$f(x) = K_{-N}(\lambda) f(x_{-N}) + \dots + K_0(\lambda) f(x_0) + \dots + K_N(\lambda) f(x_N) \quad \text{Eq. (B.10)}$$

where  $\lambda = (x - x_0)/h$  and  $h$  is the spacing between points. It may be shown (Ref. 11) that, for instance,

$$K_{-1}(\lambda) = -\frac{1}{2}[\lambda - \lambda^2], \quad K_0(\lambda) = 1 - \lambda^2, \quad K_1(\lambda) = \frac{1}{2}[\lambda^2 + \lambda^3]; \quad \text{for } N=1$$

$$K_{-2}(\lambda) = \frac{\lambda^4 - 2\lambda^3 - \lambda^2 + 2\lambda}{24}, \quad K_{-1}(\lambda) = \frac{-\lambda^4 + \lambda^3 + 4\lambda^2 - 4\lambda}{6}$$

$$K_0(\lambda) = \frac{\lambda^4 - 5\lambda^2 + 4}{4}, \quad K_1(\lambda) = \frac{-\lambda^4 - \lambda^3 + 4\lambda^2 + 4\lambda}{6}$$

$$K_2(\lambda) = \frac{\lambda^4 + 2\lambda^3 - \lambda^2 - 2\lambda}{24}; \quad \text{for } N=2.$$

Eqs. (B.11)

Tables are available for the  $K$ 's vs.  $\lambda$ , but if  $\lambda$  is irrational it might be easier to use these formulas directly. In cases where the given points are not equally spaced, one still can devise appropriate interpolation procedures which are similar but somewhat more tedious. To illustrate the application of the above, consider a spanwise station of the wing having six equally spaced chordwise stations 1, ..., 6 where the slopes  $\theta_i$  are known (see Fig. B.3). It is required to find the slopes at other points 7, ..., 5 as shown in the figure. Assume that the slope at point 7 may be adequately computed using a three-point interpolation, i.e.,  $N=1$ .

**CONFIDENTIAL**

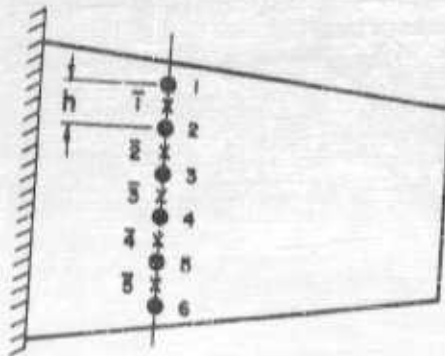


Fig. B.3 Lagrangian interpolation for a Function of One Variable

Then one can write for the deflections at the new points  $\bar{1}, \dots, \bar{5}$

$$\theta_{\bar{1}} = K_{-1}(\lambda_{\bar{1}})\theta_1 + K_0(\lambda_{\bar{1}})\theta_2 + K_1(\lambda_{\bar{1}})\theta_3$$

⋮

$$\theta_{\bar{4}} = K_{-1}(\lambda_{\bar{4}})\theta_4 + K_0(\lambda_{\bar{4}})\theta_5 + K_1(\lambda_{\bar{4}})\theta_6$$

⋮

or in matrix notation,

Eqs. (B.12)

$$\{\theta_{\bar{i}}\} = [K(\lambda_{\bar{i}})]\{\theta_i\}$$

Eq. (B.13)

where  $\{\theta_{\bar{i}}\}$  and  $\{\theta_i\}$  are column matrices,

$$[K(\lambda_{\bar{i}})] = \begin{bmatrix} K_{-1}(\lambda_{\bar{1}}) & K_0(\lambda_{\bar{1}}) & K_1(\lambda_{\bar{1}}) & 0 & 0 & 0 \\ 0 & K_{-1}(\lambda_{\bar{2}}) & K_0(\lambda_{\bar{2}}) & K_1(\lambda_{\bar{2}}) & 0 & 0 \\ 0 & 0 & K_{-1}(\lambda_{\bar{3}}) & K_0(\lambda_{\bar{3}}) & K_1(\lambda_{\bar{3}}) & 0 \\ 0 & 0 & 0 & K_{-1}(\lambda_{\bar{4}}) & K_0(\lambda_{\bar{4}}) & K_1(\lambda_{\bar{4}}) \\ 0 & 0 & 0 & K_{-1}(\lambda_{\bar{5}}) & K_0(\lambda_{\bar{5}}) & K_1(\lambda_{\bar{5}}) \end{bmatrix}$$

Eq. (B.14)

**CONFIDENTIAL**

# CONFIDENTIAL

and

$$\lambda_1 = \frac{x_1 - x_2}{h}, \dots, \lambda_4 = \frac{x_4 - x_5}{h}, \lambda_5 = \frac{x_5 - x_6}{h} \quad \text{Eq. (B.15)}$$

In a Mach box grid system, if the Mach number is changed while keeping the spanwise dimension of each box fixed as recommended in Section III, the control points will change position in the chordwise direction only. Therefore, the type of interpolation matrix illustrated above is sufficient to determine the slopes at the new control points in terms of the known slopes of the original set of fixed points (for the initial Mach number). In instances when there are fewer than three points for interpolation, such as near the tip of a delta wing, a lower-order interpolation must be resorted to.

## B.4 Lagrangian Interpolation for a Function of Two Variables

To obtain the proper interpolation for a function of two variables, the above technique may be used repeatedly. Two such examples are: (1) when the force-displacement structural influence coefficients  $C_{ij}$  (which is dependent on the two control points  $i, j$ ) are to be found at different chordwise points for given spanwise stations (see below), and (2) when the deflections and slopes are needed at points  $(x, y)$  for which  $x, y$  do not lie on the spanwise or chordwise locations of the discrete points with known deflections and slopes. (In the previous section, the  $y$ -coordinate of the new points coincided with the  $y$ -coordinate of the old points, so that the interpolation was in the stream direction only.)

As an illustration of case (1) above, let  $i$  (or  $j$ ) define the original set of points and  $i'$  (or  $j'$ ) define the new set. Bearing in mind that  $i$  and  $i'$  (or  $j$  and  $j'$ ) are restricted to the same spanwise location for this example (Fig. B.4), one obtains

$$[C_{i'j'}] = [K(\lambda_{i'})][C_{ij}] \quad \text{Eq. (B.16)}$$

and

$$\begin{aligned} [C_{i'j'}] &= [C_{ij}][K(\lambda_{i'})]^T \\ &= [K(\lambda_{i'})][C_{ij}][K(\lambda_{i'})]^T \end{aligned} \quad \text{Eq. (B.17)}$$

# CONFIDENTIAL

where  $[ \quad ]^T$  indicates the transpose of the matrix. Referring to Fig. B.4,

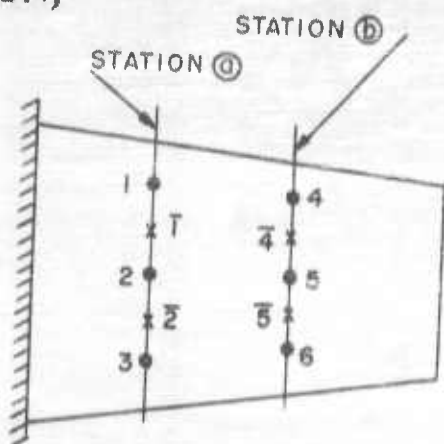


Fig. B.4 Lagrangian Interpolation for a Function of Two Variables

$$[K(\lambda_T)] = \begin{bmatrix} K_{-1}(\lambda_T) & K_0(\lambda_T) & K_1(\lambda_T) \\ K_{-1}(\lambda_z) & K_0(\lambda_z) & K_1(\lambda_z) \end{bmatrix}$$

$$[C_{ij}] = \begin{bmatrix} C_{14} & C_{15} & C_{16} \\ C_{24} & C_{25} & C_{26} \\ C_{34} & C_{35} & C_{36} \end{bmatrix}, \quad [K(\lambda_j)]^T = \begin{bmatrix} K_{-1}(\lambda_4) & K_{-1}(\lambda_5) \\ K_0(\lambda_4) & K_0(\lambda_5) \\ K_1(\lambda_4) & K_1(\lambda_5) \end{bmatrix} \quad \text{Eq. (B.18)}$$

Eqs. (B.19a-b)

# CONFIDENTIAL

Therefore one obtains for the new set of influence coefficients

$$\begin{aligned}
 [C_{ij}] &= \begin{bmatrix} C_{14} & C_{15} \\ C_{24} & C_{25} \end{bmatrix} \\
 &= \begin{bmatrix} K_-(\lambda_1) & K_0(\lambda_1) & K_+(\lambda_1) \\ K_-(\lambda_2) & K_0(\lambda_2) & K_+(\lambda_2) \end{bmatrix} \begin{bmatrix} C_{14} & C_{15} & C_{16} \\ C_{24} & C_{25} & C_{26} \\ C_{34} & C_{35} & C_{36} \end{bmatrix} \begin{bmatrix} K_-(\lambda_4) & K_+(\lambda_4) \\ K_0(\lambda_4) & K_0(\lambda_4) \\ K_-(\lambda_5) & K_+(\lambda_5) \end{bmatrix}
 \end{aligned}$$

Eq. (B.20)

The above procedure may be repeated for all other spanwise stations  $\textcircled{4}$  and  $\textcircled{5}$  to obtain the complete set of influence coefficients.

For case (2) above, the situation is somewhat different. It entails interpolation in one direction, say  $y$ -direction, keeping  $x$  constant, followed by interpolation in the other direction ( $x$ -direction), keeping  $y$  constant.

# CONFIDENTIAL

## APPENDIX C

### RECOMMENDED INTEGRATION TECHNIQUES FOR GENERALIZED FORCES

Once the downwash distributions are determined according to Appendix B, the recommended box scheme may be used to find the pressure (or the velocity potential) distribution associated with each assumed mode. Then the generalized forces are obtained by integrations over the planform of the pressure (or the velocity potential) distribution weighted with the various mode shapes.

The pressure distribution along a streamwise strip in the supersonic region of a planform is continuous and smoothly varying. To evaluate the chordwise portion of the double integral representing a generalized force, a simple integration scheme such as the rectangular rule will suffice. However, when a streamwise strip includes a segment of the mixed wingtip region, the chordwise pressure distribution exhibits a sharp drop and a discontinuity in slope across the Mach line. If many boxes were included along this strip, the segment between the Mach line and the succeeding downstream point (i.e., the segment containing the sharp drop in pressure distribution) contributes only a small fraction of the integral across the entire chord. Hence the error introduced will be small if the rectangular rule is used. However, if there are only a few boxes present (say six or less) across a streamwise strip in the mixed region, the contribution to the total force due to the sharp drop in pressure distribution may be appreciable. A refinement in the chordwise integration procedure is then recommended.

#### C.1 Refined Chordwise Integration Scheme (PIC-Method)

Referring to the planform of Fig. C.1a, a typical chordwise pressure distribution for section A-A is shown in Fig. C.1b.

From points  $c$  to  $2$  and  $3$  to  $d$ , where no sharp drop occurs, the simple rectangular rule may be applied. Between points  $2$  and  $3$ , the following integration technique is suggested: let the pressure distribution between points  $2$  and  $3$  be represented by:

$$p(x) \approx p_2 \left(1 - \sqrt{\frac{x-x_2}{l_1}}\right) + p_3 \left(\sqrt{\frac{x-x_2}{l_1}}\right) \quad \text{Eq. (C.1)}$$

where  $l_1$  is the length from point  $2$  and  $3$ . This expression yields the correct pressures at  $2$  and  $3$ , and has an infinite slope at  $2$ . The infinite slope condition is imposed because it represents the correct behavior, as may be derived from

# CONFIDENTIAL

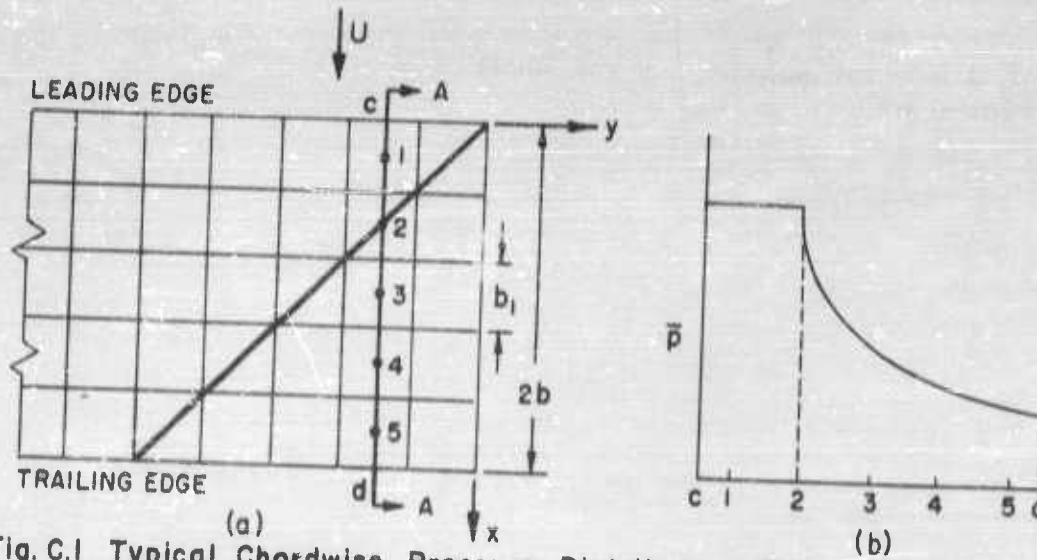


Fig. C.1 Typical Chordwise Pressure Distribution Near a Side Edge (Steady-State Condition)

steady-state results. Integrating  $p(x)$  between points 2 and 3, the formula for the lift in that segment is

$$\begin{aligned} \Delta l &= \int_{x_2}^{x_3} p(x) dx \\ &\cong \frac{b_1}{3} (p_2 + 2p_3) \end{aligned} \tag{C.2}$$

The above integration in conjunction with the rectangular rule for segments other than 2-3, yields the lift per unit span at A-A

$$\begin{aligned} l &= \int_0^{2b} p(x) dx \\ &\cong b_1 p_1 + b_1 \left(\frac{p_2}{2}\right) + \frac{b_1}{3} (p_2 + 2p_3) + b_1 \left(\frac{p_3}{2}\right) + b_1 p_4 + b_1 p_5 \\ &= b_1 \left( p_1 + \frac{5}{6} p_2 + \frac{7}{6} p_3 + p_4 + p_5 \right) \end{aligned} \tag{C.3}$$

This refined integration formula is very similar to the rectangular rule, and its use is no more difficult than the simpler rule.

# CONFIDENTIAL

In a similar manner, if the moment about any axis  $x_a$  is represented by

$$\Delta m \approx \int_{x_2}^{x_3} \left[ b_2 \left( 1 - \sqrt{\frac{x-x_2}{b_1}} \right) + b_3 \left( \sqrt{\frac{x-x_2}{b_1}} \right) \right] (x-x_a) dx \quad \text{Eq. (C.4)}$$

there results the moment expression for the segment 2-3

$$\Delta m \approx b_1 \left[ b_2 \left( \frac{7}{30} x_2 + \frac{1}{10} x_3 - \frac{1}{3} x_a \right) + b_3 \left( \frac{4}{15} x_2 + \frac{2}{5} x_3 - \frac{2}{3} x_a \right) \right] \quad \text{Eq. (C.5)}$$

The above procedure can be extended for the calculation of the generalized forces. If the weighted integration between points 2 and 3 is given by (assuming linear variation of the weighting factor between 2 and 3)

$$\Delta F = \int_{x_2}^{x_3} b(x) f(x) dx \approx \int_{x_2}^{x_3} \left[ b_2 \left( 1 - \sqrt{\frac{x-x_2}{b_1}} \right) + b_3 \left( \sqrt{\frac{x-x_2}{b_1}} \right) \right] \left[ f(x_2) \frac{x-x_2}{b_1} + f(x_3) \frac{x_3-x}{b_1} \right] dx \quad \text{Eq. (C.6)}$$

then this approximation yields

$$\Delta F = b_1 \left[ b_2 \left( \frac{7}{30} f(x_2) + \frac{1}{10} f(x_3) \right) + b_3 \left( \frac{4}{15} f(x_2) + \frac{2}{5} f(x_3) \right) \right] \quad \text{Eq. (C.7)}$$

It should be emphasized here that this refinement must be used only when there are no severe fluctuations of the pressure across the chord. This fact limits its use to planforms with supersonic leading edges. For planforms with subsonic leading edges, the whole planform is influenced by the diaphragm region, and then one must take a sufficiently large number of boxes and use the rectangular rule.

## C.2 The Determination of Generalized Forces (PIC-Method)

A generalized force is given as a double integral over the planform of the pressure of mode  $i$  weighted with the deflection function of a mode  $j$ . For instance, in dimensional coordinates

$x, y$

$$Q_{ij} = \iint_S \Delta p_i(x, y) f_j(x, y) dx dy \quad \text{Eq. (C.8)}$$

The integral over the chord at any spanwise station  $y_n$  is

# CONFIDENTIAL

$$\int \Delta p_c(x, y_n) f_j(x, y_n) dx \cong \sum_{m=1}^M a_m(y_n) \{ \Delta p_c(x_m, y_n) f_j(x_m, y_n) \} \quad \text{Eq. (C.9)}$$

where  $a_m(y_n)$  are the adjusted integration coefficients of the previous section. In cases where the rectangular rule is sufficient, the  $a_m(y_n)$  will be equal to the box dimension  $b_j$  except for boxes at the trailing edge where some sort of an area correction is recommended (cf. Rule 4, Section III.1). In addition, a spanwise numerical integration yields the generalized force

$$Q_{ij} \cong \sum_{n=1}^N \sum_{m=1}^M d_n a_m(y_n) \{ \Delta p_c(x_m, y_n) f_j(x_m, y_n) \} \quad \text{Eq. (C.10)}$$

where  $d_n$ 's are the spanwise integration constants. If here the rectangular rule is used, the  $d_n$ 's are all constants and are equal to the spanwise width of the strip ( $b_j/\rho$ ).

### C.3 The Determination of Generalized Forces (VIC-Method)

Using the pressure-velocity potential relation

$$\Delta p = \frac{\rho U}{\tau} \left[ ik \Delta \varphi + \tau \frac{\partial(\Delta \varphi)}{\partial x} \right] \quad \text{Eq. (C.11)}$$

the expression for the generalized force [Eq. (C.8)] may be put in the form

$$Q_{ij} = \frac{\rho U}{\tau} \iint_S [ ik \Delta \varphi_c(x, y) f_j(x, y) dx dy + \frac{\rho U}{\tau} \iint_S \tau \frac{\partial(\Delta \varphi_c(x, y))}{\partial x} f_j(x, y) dx dy \quad \text{Eq. (C.12)}$$

A partial integration with respect to  $x$  for the second area-integral yields

$$Q_{ij} = \frac{\rho U}{\tau} \iint_S \Delta \varphi_c(x, y) \left[ ik f_j(x, y) - \tau \frac{\partial f_j(x, y)}{\partial x} \right] dx dy + \rho U \int_{span} (\Delta \varphi_c(x_c, y)) f_j(x_c, y) dy \quad \text{Eq. (C.13)}$$

# CONFIDENTIAL

where the subscript  $t$  refers to the trailing edge at  $y$ . Here one may use the rectangular rule for both the  $x$ - and  $y$ -integrations, with the result

$$Q_y \approx \rho V \sum_{n=1}^N d_n \left\{ \Delta y_i(x_i, y_n) f_j(x_i, y_n) + \frac{1}{t} \sum_{m=1}^M a_m(y_n) \Delta y_i(x_i, y_n) \left[ t_k f_j(x_m, y_n) - b \left( \frac{\partial f_j}{\partial x} \right)_{x_m, y_n} \right] \right\} \quad \text{Eq. (C.14)}$$

Here  $d_n = b_i / \beta$  and  $a_m(y_n) = t_i$  except near the trailing edge where they must be adjusted to comply with the area correction rule (cf. Rule 4, Section III.1).

# CONFIDENTIAL

## APPENDIX D

### FORMULATION OF THE FLUTTER PROBLEM

It has been common practice in the past to apply in a flutter analysis as a series of related but separate problems. The flutter mode is assumed to be some linear combination of the first few free vibration modes of the structure. These vibration modes are calculated by whatever method is feasible. Next the aerodynamic problem is solved to provide the necessary generalized forces associated with the assumed modes. If two-dimensional forces are to be employed, as in cases of large-aspect-ratio surfaces (Ref. 12), this step is considerably simplified. With these results available, the flutter equations of motion may be formulated and solved in any of a number of possible ways. This procedure has been very successful for planforms which are rigid in the streamwise direction, i.e., the streamwise slope at any spanwise station is constant for any one of the assumed modes. A beam-rod type structure falls in this category. Experience has shown that even rather approximate assumptions as to the mode shapes and knowledge of the free uncoupled vibration frequencies of these modes usually yield satisfactory solutions. However, when plate type structures, such as delta wings, are to be analyzed, accurate representations of the assumed modes become necessary.

Another approach is a direct integral equation formulation for the flutter problem in terms of aerodynamic and structural influence coefficients (Ref. 13), but this method does not offer all of the advantages in simplicity obtained from the assumed mode technique.

#### D.1 Equations for Bending-Torsion-Aileron Flutter

If the structure to be analyzed is of the conventional beam-rod type, the formulation according to the present report is very similar to the method presented in Ref. 12 with the sole exception that the generalized forces are evaluated by the aerodynamic influence coefficient method (the notations are those of Ref. 12, except that the spanwise variable is taken to be  $y$ ):

# CONFIDENTIAL

$$\bar{A} = \left[ 1 - \left( \frac{\omega_k}{\omega} \right)^2 \left( \frac{\omega_p}{\omega_k} \right)^2 (1 + i q_R) \right] \int_0^L M [f_R(y)]^2 dy + \frac{1}{\omega^2} Q_{RR}$$

$$\bar{B} = \int_0^L S_\alpha [f_R(y)] [f_\alpha(y)] dy + \frac{1}{\omega^2} Q_{\alpha R}$$

$$\bar{C} = \int_{L_1}^{L_4} S_\rho [f_R(y)] [f_\rho(y)] dy + \frac{1}{\omega^2} Q_{\rho R}$$

$$\bar{D} = \int_0^L S_\alpha [f_R(y)] [f_\alpha(y)] dy + \frac{1}{\omega^2} Q_{R\alpha}$$

$$\bar{E} = \left[ 1 - \left( \frac{\omega_k}{\omega} \right)^2 (1 + i q_\alpha) \right] \int_0^L I_\alpha [f_\alpha(y)]^2 dy + \frac{1}{\omega^2} Q_{\alpha\alpha}$$

$$\bar{F} = \int_{L_1}^{L_4} [I_\rho + (c-a) b S_\rho] [f_\alpha(y)] [f_\rho(y)] dy + \frac{1}{\omega^2} Q_{\rho\alpha}$$

$$\bar{G} = \int_{L_1}^{L_4} S_\rho [f_R(y)] [f_\rho(y)] dy + \frac{1}{\omega^2} Q_{R\rho}$$

$$\bar{H} = \int_{L_1}^{L_4} [I_\rho + (c-a) b S_\rho] [f_\alpha(y)] [f_\rho(y)] dy + \frac{1}{\omega^2} Q_{\rho\alpha}$$

$$\bar{I} = \left[ 1 - \left( \frac{\omega_k}{\omega} \right)^2 \left( \frac{\omega_p}{\omega_k} \right)^2 (1 + i q_\rho) \right] \int_{L_1}^{L_4} I_\rho [f_\rho(y)]^2 dy + \frac{1}{\omega^2} Q_{\rho\rho}$$

Eq. (D.1 a-1)

# CONFIDENTIAL

Typical examples of the generalized forces in these equations are listed below:

$Q_{\beta h}$  = the weighted lift due to unit amplitude of bending motion at the reference station,

$$= \int_0^L \Delta l_h [f_h(y)] dy, \quad (h=1 \text{ at the reference station}),$$

$Q_{\alpha\alpha}$  = the weighted moment about the elastic axis due to unit amplitude of pitching motion at the reference station,

$$= \int_0^L (\Delta m_{\alpha})_{e.a.} [f_{\alpha}(y)] dy,$$

and

$Q_{\beta\alpha}$  = the weighted moment about the elastic axis due to unit amplitude of aileron motion at the reference station,

$$= \int_{L_1}^{L_2} (\Delta m_{\beta})_{e.a.} [f_{\alpha}(y)] dy,$$

where  $(\quad)_{e.a.}$  denotes a moment about the elastic axis. The spanwise running lifts and moments, such as  $\Delta l_h$ ,  $(\Delta m_{\alpha})_{e.a.}$  and  $(\Delta m_{\beta})_{e.a.}$  etc. may be obtained by appropriate chordwise integrations of the pressures or of the velocity potentials which are calculated in advance by the box scheme. Finally, spanwise integrations may be carried out by numerical means. The quantities  $\bar{A}, \dots, \bar{I}$  are the elements of the flutter determinant

$$\begin{vmatrix} \bar{A} & \bar{B} & \bar{C} \\ \bar{D} & \bar{E} & \bar{F} \\ \bar{G} & \bar{H} & \bar{I} \end{vmatrix}$$

Associated with this determinant are two unknowns (such as the velocity and the frequency). At flutter these two unknowns (eigenvalues) are such that the value of the determinant is zero.

# CONFIDENTIAL

## D.2 Flutter Equations for Plate-Type Structures

For low-aspect-ratio surfaces or plate-type structures, the assumption of beam-rod type deformations is no longer justified. A new approach must be devised to treat these cases. As an example of the modified procedure, consider a cantilever triangular wing which is divided into ten areas as shown in Fig. D.1. Each such area has a mass  $m_n$  concentrated at its center-of-gravity location  $(x_n, y_n)$ . If the structural influence coefficients

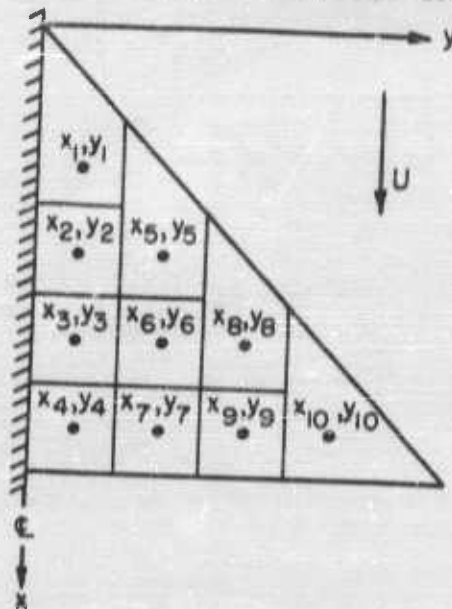


Fig. D.1 A Delta Wing Configuration with Lumped Masses

associated with these points are given, one may obtain by matrix iteration (Ref. 14) the first few free vibration frequencies and the related orthogonal mode shapes. Once they are available, one may proceed to the flutter equations of motion. If the flutter mode is assumed to consist of the first two free vibration modes  $A(t)f_1(x, y)$  and  $B(t)f_2(x, y)$  then the displacement of a point  $(x_n, y_n)$  may be written as

$$z_n(t) = A(t)f_1(x_n, y_n) + B(t)f_2(x_n, y_n) \quad \text{Eq. (D.2)}$$

For use in deriving Lagrange's equations, the total kinetic energy of the system is

# CONFIDENTIAL

$$\begin{aligned}
 KE &= \frac{1}{2} \sum_{n=1}^{10} m_n \dot{z}_n^2 \\
 &= \frac{1}{2} \dot{A}^2 \sum_1^{10} m_n [f_1(x_n, y_n)]^2 + \frac{1}{2} \dot{B}^2 \sum_1^{10} m_n [f_2(x_n, y_n)]^2 + \dot{A} \dot{B} \sum_1^{10} m_n [f_1(x, y)] [f_2(x, y)]
 \end{aligned}$$

Eq. (D.3)

Since the last term is zero by the orthogonality condition, the kinetic energy terms in Lagrange's equations are

$$\frac{d}{dt} \left( \frac{\partial(KE)}{\partial \dot{A}} \right) = \ddot{A}(t) \sum_1^{10} m_n [f_1(x_n, y_n)]^2$$

$$\frac{d}{dt} \left( \frac{\partial(KE)}{\partial \dot{B}} \right) = \ddot{B}(t) \sum_1^{10} m_n [f_2(x_n, y_n)]^2$$

Eqs. (D.4a-b)

For simple harmonic motion,  $\ddot{A}(t) = -\omega^2 A(t)$ ,  $\ddot{B}(t) = -\omega^2 B(t)$ . Because of the orthogonality of the modes, one may write for the potential energy terms

$$\frac{\partial(PE)}{\partial A} = \omega_1^2 A(t) \sum_1^{10} m_n [f_1(x_n, y_n)]^2$$

$$\frac{\partial(PE)}{\partial B} = \omega_2^2 B(t) \sum_1^{10} m_n [f_2(x_n, y_n)]^2$$

Eqs. (D.5a-b)

Finally, the generalized forces  $Q_A$ ,  $Q_B$  are:

$$Q_A = \iint_S \{ (\Delta p)_{Af_1} + (\Delta p)_{Bf_2} \} f_1(x, y) dx dy$$

$$= \frac{\rho U}{T} \iint_S \left\{ (ik \Delta \varphi + t \frac{\partial(\Delta \varphi)}{\partial x})_{Af_1} + (ik \Delta \varphi + t \frac{\partial(\Delta \varphi)}{\partial x})_{Bf_2} \right\} f_1(x, y) dx dy = A Q_{AA} + B Q_{BA}$$

Eq. (D.6a)

# CONFIDENTIAL

$$\begin{aligned}
 Q_B &= \iint_S \{ (\Delta p)_{Af} + (\Delta p)_{Bf} \} f_2(x,y) dx dy \\
 &= \frac{\rho U}{t} \iint_S \left\{ (iR\Delta\varphi + t \frac{\partial(\Delta\varphi)}{\partial x})_{Af} + (iR\Delta\varphi + t \frac{\partial(\Delta\varphi)}{\partial x})_{Bf} \right\} f_2(x,y) dx dy = A Q_{AB} + B Q_{BA}
 \end{aligned}$$

Eq. (D.6b)

where for instance  $(\Delta p)_{Af}$  indicates the pressure distribution due to the motion  $A(t)f_1(x,y)$  and the integrations are over the planform  $S$ . The task of evaluating these forces is discussed in Appendix C.

Equations (D.4a-b), (D.5a-b), and (D.6a-b) provide the elements in Lagrange's equations

$$\frac{d}{dt} \left( \frac{\partial(KE)}{\partial \dot{q}_r} \right) + \frac{\partial(PE)}{\partial q_r} = Q_r, \quad q_r = A, B. \quad \text{Eqs. (D.7)}$$

Equations (D.7) form a set of two simultaneous homogeneous linear equations in the complex modal amplitude functions  $A$  and  $B$ :

$$\begin{bmatrix}
 (\omega^2 - \omega_1^2) \sum_1^{10} m_n [f_1(x_n, y_n)]^2 + Q_{AA} & Q_{BA} \\
 Q_{AB} & (\omega^2 - \omega_2^2) \sum_1^{10} m_n [f_2(x_n, y_n)]^2 + Q_{BB}
 \end{bmatrix}
 \begin{Bmatrix}
 A \\
 B
 \end{Bmatrix}
 = 0.$$

Eq. (D.8)

The condition for flutter is that the determinant of the above matrix should vanish.